Heterogeneity in the Effects of Neighborhood Deprivation on Economic Decision Making and Mental Health in Children

Junghoon Park[1], Minje Cho[2], Eunji Lee[3], Bo-Gyeom Kim[3], Gakyung Kim[4], Yoonjung Yoonie Joo[5], Jiook Cha* [3, 4, 6]

1. Interdisciplinary Program in Artificial Intelligence, College of Engineering, Seoul National University, Seoul, South Korea
2. Department of Economics, Korea University, Seoul, South Korea
3. Department of Psychology, College of Social Sciences, Seoul National University, Seoul, South Korea
4. Department of Brain and Cognitive Sciences, College of Natural Sciences, Seoul National University, Seoul, South Korea
5. Institute of Data Science, Korea University, Seoul, South Korea
6. Graduate School of Data Science, Seoul National University, South Korea

*Corresponding Author: Jiook Cha, PhD

Gwanak-ro 1, Building 16, Suite M512, Gwanakgu, Seoul, 08826, South Korea

Email: connectome@snu.ac.kr

Author Contributions: J.P. and J.C. designed research; J.P. and M.C. performed research; J.P., M.C., E.L., B.-G.K., G.K., Y.Y.J. analyzed data; and J.P., M.C., and J.C. wrote the paper.

Competing Interest Statement: Authors have no competing interests.

Classification: Biological Sciences/Psychological and Cognitive Sciences, Social Sciences/Psychological and Cognitive Sciences

Keywords: Intertemporal reward valuation, Psychotic-like experiences, Causal machine learning, Childhood socioeconomic environment, Heterogeneous treatment effects

This PDF file includes:

Main Text
Figures 1 to 4
Tables 1 to 2

Abstract

Delay discounting is linked to developmental trajectories of cognition and the brain, as well as psychopathology, such as psychosis. Although childhood socioeconomic deprivation is associated with both increased delay discounting and a higher incidence of psychotic disorders, the genetic and neural basis of these associations remains unclear. This study examined the causal relationships between neighborhood socioeconomic deprivation, delay discounting, and psychotic-like experiences (PLEs) in 2,135 preadolescent children using machine learning-based causal inference methods. We found that neighborhood deprivation, as measured by the Area Deprivation Index, had significant causal effects on delay discounting (β= -1.7297, p-FDR= 0.0258) and 1-year and 2-year follow-up PLEs (β= 1.3425~1.8721, p-FDR$\leq$ 0.0291). Furthermore, our analysis revealed significant heterogeneous causal effects of neighborhood deprivation on PLEs (p-FDR<0.005). The subgroups most vulnerable to these causal effects exhibited steeper discounting of future rewards, higher polygenic scores for educational attainment, reduced structural volume/area/white matter in the parahippocampal, right temporal pole, and right pars opercularis, and greater functional activation in the limbic system during Monetary Incentives Delay tasks. Our findings highlight the importance of a bioecological framework and the involvement of the mesocorticolimbic system in the causal relationship between socioeconomic deprivation and the risk of psychosis during childhood. Overall, our results support that enhancing the residential socioeconomic environment could positively influence child development.

Significance Statement

Discerning the complex interplay of genetic, neural, and environmental factors within the relationship between childhood environment and psychopathology is essential for developing personalized health care. To provide optimal health care for each patient, identifying the biological and socioeconomic characteristics of the most vulnerable population is necessary. Through the application of state-of-the-art causal machine learning methods, this study shows that children with genetic and neural associates of impatient reward valuation are at a heightened risk of developing psychosis when exposed to neighborhood socioeconomic adversity. These findings underscore the significance of enhancing the childhood environment as a means to address social and health disparities.

Introduction

In *Critique of Practical Reason*, Immanuel Kant posits the inherent power of human reason, asserting that it is an a priori capacity independent of external factors, enabling individuals to engage in responsible actions (1). However, contemporary scientific research conducted over the past several decades has accumulated considerable evidence that challenges the assertions of this 18th-century philosopher. Specifically, the environment in which individuals develop exerts a substantial influence on their identities and actions.

Adverse childhood environments, such as low family income, inadequate nutrition, physical or sexual abuse, and unsafe neighborhoods, have been correlated with an elevated risk of pathologies, including schizophrenia (2-4), impoverished cognitive ability (5-7), anxiety, bipolar disorder, self-harm, depression (3, 4, 8), substance abuse, and obesity (9, 10). Furthermore, these environments are associated with negative social outcomes, such as poor academic performance (11, 12), low income, unemployment (13-18), incarceration, teen pregnancy (19). Additionally, childhood adversity has been linked to risky behaviors, encompassing criminal activity (20), excessive consumption of calorie-dense foods (21), substance use (22, 23), deficient self-control (24), and disrupted reward processing (25).

But what is the complex correlation between adverse childhood environment, irresponsible behavior, and negative social and health outcomes? We hypothesized that childhood adversity causes impairment in one's valuation system, leading to negative life outcomes. Children who experienced social adversities such as poverty show steeper discounting of future rewards in adulthood and have greater risk of psychosis (2, 3, 26-28).

Lower socioeconomic status positively correlates with functional brain activity concordance and grey matter volume within reward-related areas (i.e., ventral striatum, putamen, caudate nucleus, orbital frontal cortex) and negatively with executive-related areas (i.e., frontal, medial frontal cortex) (29). A recent study reported that neuroanatomical features including total cortical volume, surface area, and thickness mediates the association of environmental risk factors and psychotic-like experiences (PLEs) in children (3).

In addition, individuals with steeper discounting of future rewards (i.e., value present rewards much higher than future rewards) were inclined to save less, invest less in education, more likely to engage in criminal behavior, exhibit lower academic performance, and have less economic wealth (30-33). Impairment of the intertemporal valuation system is associated with psychiatric disorders, including schizophrenia, attention deficit/hyperactivity disorder (ADHD), Parkinson's disease, and drug addiction (34, 35). Particularly, schizophrenia can be seen as an aberrant neural response towards irrelevant rewards due to increased tonic dopamine (34, 36-38). Blunted dopaminergic projections from the ventral tegmental area to the mesocorticolimbic regions disrupt reward anticipation and perception (36, 37), causing delusions or hallucinations. This is supported by consistent reports of steeper delay discounting in schizophrenia patients (39-41).

In the present study, our primary objective was to investigate the causal impact of neighborhood socioeconomic deprivation on adolescents' delay discounting, which pertains to individuals' intertemporal decision-making and impulsive behavior, as evidenced by the extent to which they discount future rewards. Additionally, this study aimed to investigate the impact of such deprivation on adolescents' psychotic-like experiences (PLEs). Exposure to adversities at the neighborhood level during childhood has been shown to negatively

influence neurocognitive development, subsequently resulting in psychiatric disorders and unfavorable social outcomes, such as decreased income, reduced probability of college attendance, and limited employment opportunities (3, 7, 17, 28, 42-45). This phenomenon is particularly pronounced in societies where discrimination based on family income or race/ethnicity restricts underprivileged families from selecting neighborhoods that present greater opportunities for upward social mobility, as observed in the United States (17).

It is crucial to note that PLEs, which are considered as a clinically significant risk indicator for schizophrenia and general psychopathology (2, 3, 46), exhibit the strongest association with environmental risk factors in comparison to other internalizing/externalizing symptoms during early adolescence (3). The present study endeavors to contribute to a deeper understanding of the potential causal mechanisms underlying these associations, with the aim of informing policy and intervention strategies.

Our second aim was to test whether the causal effects of neighborhood deprivation on children's PLEs are heterogeneous based on individual's delay discounting and its genetic, neural correlates. The heterogeneous nature of psychopathology has long posed significant challenges for clinical diagnosis and treatment (47, 48). Given that the genetic and neural correlates of delay discounting substantially overlap with those of schizophrenia (38, 49, 50), the shared biological foundations between reward valuation and schizophrenia may result in heterogeneous effects of environmental exposure on an individual's psychotic symptoms. By investigating these potential variations, this study seeks to enhance the understanding of the complex interplay between environmental factors and individual predispositions in the development of psychopathology.

Identifying heterogeneity of treatment/exposure is crucial for the development of personalized health care. Delivering optimal health care for each patient necessitates the recognition of genetic markers and demographic characteristics associated with individual variations in treatment effects (51, 52). However, previous studies employing traditional methods of testing treatment effect heterogeneity have often been unsuccessful in discerning the intricate interplay between genetic and environmental factors (53, 54). Linear models with interaction terms of features selected a priori by the researcher may not fully reflect the complex and elusive gene-environment interplay, particularly in genetic and neuroscience research where the input features are usually high dimensional.

To address this knowledge gap, the present study employed an inductive approach to assess heterogeneous treatment effects using a state-of-the-art nonparametric causal machine learning algorithm. Furthermore, the study utilized multimodal magnetic resonance imaging (MRI) data from 11,876 preadolescent children aged 9 to 12 years old, who participated in the Adolescent Brain Cognitive Development (ABCD) Study. The ABCD Study represents the largest longitudinal investigation of children's neurodevelopment in the United States. By integrating innovative analytical techniques and a large, diverse sample, this study aims to advance the understanding of the complex interactions between genetic and environmental factors, ultimately contributing to the development of more effective personalized health care strategies.

Results

The demographic characteristics of the final sample (N=2,135) are presented in **Table 1**. Within the sample, 46.14% were female and 53.86% were male, 76.63% of participants had married parents, the mean family income was $70,245, and 65.57% identified their race/ethnicity as white. To ensure the representativeness of the final sample, a supplementary table comparing the sample's demographic characteristics with those of the general United States population is provided in the SI Appendix (**Table S1**). This comparison serves to reinforce the validity and generalizability of the study's findings.

A non-randomized observational study, such as the ABCD study, greatly benefits from rigorous confound modeling when examining associative and causal relationships among variables. For example, GPS, environmental variables, and phenotypic outcomes often share common unobserved causes (55). We used instrumental variable (IV) regression to adjust for unobserved confounding bias in identifying the unbiased causal effects of neighborhood socioeconomic adversity (measured with *Area Deprivation Index*, henceforth ADI) on delay discounting and PLEs (56). Utilizing such a methodological approach contributes to the robustness of the findings and enhances the validity of the study's conclusions.

In an initial exploratory analysis, conventional linear instrumental variable (IV) regression (56) was conducted to identify potential causal effects of the Area Deprivation Index (ADI) on various neurocognitive, behavioral, and psychiatric outcomes, including cognitive intelligence, depression, and bipolar disorder. Among all the assessed outcomes, delay discounting and PLEs demonstrated significant causal associations with ADI **(*SI Appendix*, Table S2)**. This preliminary analysis provided a foundation for further

investigation into the causal relationships between neighborhood socioeconomic adversity and these specific outcomes.

Average Treatment Effects of Neighborhood Socioeconomic Adversity on Delay Discounting and PLEs

In the primary analyses, we used IV random forest (henceforth, IV Forest) (57, 58) to obtain nonparametric, doubly robust estimates of average treatment effects of ADI on delay discounting and PLEs. The IV Forest method allows us to assess non-biased causal relationships between variables that are likely nonlinear—such as environmental risks and neurocognitive development (7, 59, 60)—using non-randomized, observational data (57). IV Forest analyses revealed that a higher ADI significantly correlated with a lower delay discounting rate (β= -1.7297, p-FDR= 0.0258) and a higher PLE (β= 1.3425~1.8721, p-FDR$\leq$ 0.0291) (**Table 2**).

Supplementary analyses were conducted using an alternative causal machine learning method (i.e., *Double ML* (61, 62)) to validate the results. We built a partial-linear IV model and a nonparametric interactive IV model. The findings from both IV-based Double ML models were consistent with those obtained from the IV Forest (***SI Appendix*, Table S3**), further supporting the primary analyses and conclusions drawn from the study.

Heterogeneous Treatment Effects of Neighborhood Socioeconomic Adversity on PLEs, conditioned on the Genetic and Neural Correlates of

Delay Discounting

Next, we tested whether the impact of ADI was heterogeneous across children, and, if so, how the biological correlates of intertemporal valuation conferred the heterogeneity. Children's genetic liability and neural representation were assessed using genome-wide polygenic scores (GPS) and structural MRI and monetary incentive delay (MID) task fMRI data. To find the best subset of genetic and neural correlates of delay discounting, we first selected GPS and MRI brain regions of interest (ROIs) specifically related to delay discounting. To analyze the nonparametric correlations of multiple input variables, we used a random forest-based feature selection *Boruta* algorithm (63). Its robustness and effectiveness in selecting relevant features in high dimensional, intercorrelated biomedical data (e.g., MRI) has been validated (63) and consistently applied in genetics and neuroscience research (64-66). The variables significantly correlated with delay discounting (p-Bonferroni<0.05) were GPS of cognitive performance, IQ, and education attainment; anatomical features (e.g., surface area, volume) in the limbic system (temporal pole, parahippocampal gyrus, caudate nucleus, rostral anterior cingulate, isthmus cingulate), inferior frontal gyrus (pars opercularis), and fusiform gyrus; mean beta activations of rewards/losses versus neutral feedback in the midbrain areas (thalamus proper, ventral diencephalon), precentral gyrus, supramarginal gyrus, temporal lobe (transverse temporal gyrus, superior temporal gyrus), and insula (***SI Appendix*, Table S4**).

We then tested the heterogeneous treatment effects of ADI with the selected GPS and brain ROIs as covariates. To identify resilient/vulnerable groups, we conducted 5-fold cross-validation model fitting to obtain honest, unbiased estimates of conditional average treatment effect (CATE) and ranked observations into quintiles by the CATE estimates (Q1: most

resilient ~ Q5: most vulnerable). After 100 iterations, we tested whether the predicted ADI effect in the lowest quintile is significantly different from the others (58, 67). We found significant heterogeneity of the ADI effects on 1-year and 2-year follow-up PLEs across the five subgroups (all p-FDR<0.005) (**Fig. 1** and ***SI Appendix*, Table S5**).

To examine the role of each genetic and neural correlates within the heterogeneous effects of ADI, we obtained Shapley additive explanation (SHAP) scores (68). SHAP scores show each variable's positive or negative contribution to the differential causal effects of ADI between resilient and vulnerable groups. In the 1-year follow-up PLEs, more vulnerable subgroups of children (i.e., a greater negative impact of ADI on PLEs) had steeper discounting of future rewards, smaller right parahippocampal area and volume, smaller right temporal pole white matter and area, smaller intracranial volume, smaller right pars opercularis volume and area, smaller total grey matter volume, lower total intelligence, lower BMI, lower IQ GPS, lower cognitive performance GPS, younger parents, less likely to be Hispanic, larger right caudate volume, larger right fusiform volume, and higher educational attainment GPS. During MID tasks, regardless of the size of reward or loss, more vulnerable children had greater neural activation in the right posterior cingulate, right ventral diencephalon, left thalamus proper, and left precentral gyrus, and decreased activation in the left superior temporal gyrus. Some of these associations were reversed in the 2-year follow-up PLEs: more vulnerable children had smaller right fusiform volume, larger parahippocampal area, larger intracranial volume, and greater activation in the superior temporal gyrus, and less activation in the precentral gyrus and thalamus proper during MID tasks. They also had smaller left white surface area, lower family income, greater activation in the insula during MID tasks compared to more resilient subgroups (**Fig. 2**).

We conducted three additional analyses to validate the robustness of the results. Firstly, we built an alternative IV Forest model with GPS and brain ROIs that were jointly associated to delay discounting and PLEs. This reduced model was unable to capture the heterogeneous effects of ADI across participants as effectively as the main IV Forest model (Total Score PLEs 1-year follow-up: p-FDR>0.05) (**Fig. 3A** and ***SI Appendix*, Table S6**). Secondly, we tested whether the heterogeneous effects of neighborhood adversity varied among psychotic symptoms. ADI exhibited significant heterogeneous treatment effects across delusional PLEs and hallucinational PLEs (all p-FDR<0.005) (**Fig. 3B** and ***SI Appendix*, Table S7**). Contrary to those of hallucinational symptoms, children more vulnerable to delusional symptoms when exposed to neighborhood adversity had decreased activation in the left precentral gyrus during MID tasks, larger left white surface area, smaller isthmus cingulate area, higher family income, and lower BMI (**Fig. 4**). Lastly, we conducted linear IV mediation analyses to test whether the role of delay discounting between the causal impact of ADI on PLEs can be captured with a conventional linear mediation model (69). This model showed no significant mediation effects of delay discounting (β= -1.5266 [95% CI, -19.8003~15.25] ~ -0.3335 [95% CI, -4.1392~4.4482]) (***SI Appendix*, Table S8**).

Discussion

In this study, we examined the relationship between neighborhood socioeconomic deprivation and intertemporal choice behavior (delay discounting) as well as psychopathology in children, while considering the diverse influences of neighborhood deprivation and its underlying biological, environmental, and behavioral determinants. Our findings can be categorized into two main aspects. Firstly, a more disadvantaged neighborhood environment was associated with steeper delay discounting (lower impulse control) and higher PLEs. The association remained significant after adjusting for known, observed (e.g., familial socioeconomic status), and unobserved confounding factors. Secondly, the impact of disadvantaged neighborhood environments on PLEs was heterogeneous, depending not only on delay discounting but also on genetic propensity for cognitive capacity, family history of psychiatric disorders, and brain morphometry and functioning (task activation). The conditions identified in the causal machine learning models may represent vulnerability or resilience factors, thereby rendering the impact of neighborhood adversity heterogeneous.

Our findings hold implications for social science. Using causal machine learning models, such as IV Forest and Double ML, we provide consistent and robust evidence that residential adversity during childhood leads to steeper discounting of future rewards. This outcome challenges the prevailing assumption in economics that an individual's rate of discounting future rewards (time preference) is an exogenous parameter of intertemporal choice, given a priori, and cannot be influenced by external factors (32). Thus far, limited attention has been devoted to examining whether the development of an individual's parameter for intertemporal

choice is affected by environmental determinants (33), although one study in economics made theoretical suggestions about the endogenous nature of temporal discounting (70).

We address this knowledge gap by identifying the potential causal influence of neighborhood environment on intertemporal choice using longitudinal observations of preadolescent children aged 9-10 years—a critical period for neurocognitive development. Given that an individual's intertemporal valuation of rewards contributes to economic and health disparities between individuals (30, 34, 50), early socioeconomic deprivation may result in a behavioral poverty trap (33), wherein individuals raised in impoverished environments tend to exhibit shortsighted behavior, making it increasingly difficult to escape poverty. Economic policies promoting positive intertemporal choice (e.g., increased savings, healthy diet) have predominantly focused on paternalistic welfare policies in adulthood, based on the assumption that an individual's delay discounting is exogenous (32). Our findings suggest that policies aimed at enhancing the socioeconomic environment during childhood may foster improved intertemporal choice behavior, thereby reducing economic (33) and health inequality (23, 71).

Our second findings highlight the heterogeneous effects of the neighborhood deprivation on PLEs. Children exposed to residential deprivation with a higher risk of psychosis exhibited steeper discounting of future rewards, lower cognitive intelligence, smaller volume/area/white matter in the right parahippocampal, right temporal pole, right pars opercularis, and total grey matter, and increased activation in the limbic system (e.g., right posterior cingulate and right ventral diencephalon) during MID tasks. Additionally, children with higher risk of delusional symptoms had decreased activation in the precentral gyrus and smaller isthmus cingulate area whereas opposite associations were found in those with higher

risk of hallucinational symptoms. Although speculative, it is plausible that the influence of neighborhood deprivation on both delay discounting and the risk for psychosis targets a shared neural substrate, namely, reduced structural volume/area/white matter and heightened functional activation associated with dysregulation of glucocorticoid and dopamine, leading to an increased risk of psychosis.

Maladaptive valuation of intertemporal rewards (i.e., excessive discounting of future rewards) arises from dysregulation of the mesocorticolimbic dopaminergic system (34, 38, 41). Animal models show adverse social environments triggers chronic dysregulation of glucocorticoid signaling through epigenetic control and consequently leads to disrupted dopaminergic circuit during adolescence (72). This finding is supported by recent human studies (25, 73, 74). Childhood exposure to social adversity may contribute to psychopathology via abnormal development of the striatum and orbitofrontal cortex (dopamine pathway), and the hippocampus, amygdala, and medial prefrontal cortex (glucocorticoids pathway) (74). Young adults with a history of childhood social deprivation exhibit impaired reward processing, particularly in the cingulate, striatum, and inferior frontal gyrus (25, 73).

It is worth noting that the age of our sample (9-12 years old) corresponds to a critical period during which these mesocorticolimbic regions undergo significant changes (75, 76). Additionally, dysfunction of the dopaminergic system has been consistently implicated in psychiatric disorders such as psychosis and schizophrenia among adolescents and adults (34-38, 41, 77). Collectively, our findings on the heterogeneous effects of neighborhood deprivation contribute to the growing body of evidence suggesting that negative environmental impacts on economic decision-making and psychopathology share a common

neural basis.

We found that with the presence of residential disadvantage, children more vulnerable to having PLEs when exposed to neighborhood deprivation had lower GPS of cognitive performance and IQ, and higher educational attainment GPS. At first, this finding may seem incongruous with prior reports indicating a negative association between PLEs and educational attainment GPS (28, 78, 79).

The heterogeneous relationship between the genetic liability to educational attainment and PLE depending on the existence of residential disadvantage may be elucidated using the bioecological model and the Scarr-Rowe hypothesis of gene-environment interactions (80-82). These frameworks propose that genetic influences are attenuated in adverse environments. An analogy to this model is that in infertile soil, plants are unable to access adequate nutrients, leading to stunted growth overriding their genetic predisposition for height (83). In the absence residential disadvantage, children with higher GPS related to educational attainment exhibit increased genetic resilience against psychosis. However, exposure to residential disadvantage weakens the gene-psychosis association, and the genetic resilience is diminished. Consequently, individuals with higher educational attainment GPS experience a more significant loss of potential genetic resilience, rendering them more susceptible to the deleterious effects of ADI on PLEs.

In concordance with our findings, recent large-scale studies have demonstrated that genetic influences on brain structure, cognition, and psychopathology are less potent in adverse environments (e.g., abuse) (84, 85) and more pronounced in enriched environments (e.g., high socioeconomic status) (81, 86, 87). These studies, in conjunction with our study,

may provide novel insights into the genetic and environmental underpinning of psychopathology in children. Furthermore, while the GPS of cognitive performance and IQ are mostly related to cognitive skills, the polygenic signals of educational attainment are more widely associated with noncognitive and social skills (88), and a variety of social outcomes including social mobility (89) and wealth inequality (90). This may be the reason why the bioecological model was prominent in educational attainment GPS, but not in GPS of cognitive performance and IQ.

Our ability to identify the heterogeneous negative impact of neighborhood deprivation on childhood psychopathology was facilitated by our innovative utilization of recent rigorous causal machine learning modeling techniques. Using the IV Forest method, we found evidence that residential deprivation may exert differential effects on children's risk of psychosis, contingent upon a variety of genetic factors (e.g., GPS of cognitive performance, educational attainment, and IQ (28, 49, 78, 79)) and environmental risk factors (e.g., family income (3, 45)) previously identified in the literature. Our results were adjusted for potential biases from observed and unobserved variables. The machine learning algorithm effectively modeled the intricate patterns of gene-environment interactions. Conversely, conventional linear mediation analysis—a traditional deductive statistical approach that relies on predefined interaction terms—failed to reveal a significant mediation of delay discounting between ADI and PLEs.

The IV Forest model enables data-driven feature selection and stratification of heterogeneous treatment effects (57, 58), thereby inductively assessing nonlinear patterns of heterogeneous treatment effects not predefined by the investigator, in contrast to traditional deductive statistical approaches. Prior studies relying on the deductive approach often suffer

from low statistical power and bias (55, 91), inadequately reflecting the complexity of gene-environment interactions (53, 54). Consequently, we posit that causal modeling approaches that assess heterogeneous treatment effects hold significant potential as powerful tools for advancing precision science in psychology and medicine.

Several limitations of this study warrant consideration. First, interpretations of our findings as true causality should be approached with caution. Although we employed both conventional and state-of-the-art causal inference methods to minimize bias from unobserved variables, the ABCD study is a non-randomized, observational investigation. Second, the majority of participants identified their race/ethnicity as white (63.76%), which may limit the generalizability of our findings. However, a recent study (92) suggests that measures of temporal discounting remain robust across 61 countries worldwide (n=13,629). Third, while childhood psychotic symptoms have been associated with an increased risk of developing mental illnesses later in life (93), we did not identify significant causal effects of neighborhood deprivation on other forms of psychopathology (e.g., anxiety disorder, bipolar disorder, eating disorder, suicidal behavior, sleep problems). It is plausible that the (heterogeneous) effects of early residential adversity on psychiatric disorders other than prodromal psychosis may not become apparent until later adolescence. Lastly, future research should examine the heterogeneous effects of additional environmental risk factors, such as parenting behavior (28) and early life stress (84), to provide a more comprehensive understanding of the environmental influences on psychopathology..

This study highlights the differential effects of neighborhood disadvantage on intertemporal economic decisions and psychotic risk during early childhood. Emphasis should be placed on identifying heterogeneous treatment effects through the integration of

various genetic and environmental factors, with the aim of informing personalized health care strategies. Furthermore, we propose that enhancing the childhood environment could contribute to the reduction of economic and health inequality gaps. By addressing the root of the problem, this indirect approach may assist individuals in developing the capacity to make more informed choices, ultimately promoting better outcomes.

The insights gleaned from our novel analytical methods revive longstanding philosophical inquiries: do humans possess reason or free will independent of their environment? If not, and the capacity for responsible behavior is contingent upon one's external circumstances, how can we justify punishment for criminal and morally reprehensible actions? Addressing these questions necessitates further interdisciplinary research that encompasses multiple fields of study, illuminating the complex relationship between individual agency and environmental factors in the context of ethical and legal considerations.

Materials and methods

Study Participants

The ABCD Study recruited participants from 21 research sites across the nation, utilizing a stratified, probability sampling method to capture the sociodemographic variation of the US population (94). We used the baseline, first year, and second year follow-up datasets included in ABCD Release 4.0, downloaded on February 10, 2022.

Of the initial 11,876 ABCD samples, we removed participants without genotype data,

MRI data, NIH Toolbox Cognitive Battery, delay discounting, residential address, ADI, PLEs. As recommended by the ABCD team (95), Johnson & Bickel's two-part validity criterion (96) was used to exclude subjects with inconsistent responses (i.e., indifferent point for a given delay larger than that of an indifference point for a longer delay). Missing values of covariates were imputed using k-nearest neighbors. The final samples included 2,135 multiethnic children.

Data

Neighborhood Disadvantage

Neighborhood disadvantage was measured with Residential History Derived Scores based on the Census tracts of each respondent's primary addresses by the ABCD team. Consistent with prior research (3, 43), we chose national percentile scores of the Area Deprivation Index, calculated from the 2011~2015 American Community Survey 5-year summary. It has 17 sub-scores regarding various socioeconomic factors such as median household income, income disparity, percentage of population aged more than 25 years or more with at least a high school diploma, and percentage of single-parent households with children aged less than 18 years, etc. Higher values of the Area Deprivation Index and poverty and fewer years of residence indicate greater residential disadvantage.

Delay Discounting

Delay discounting was measured by the adjusting delay discounting task in the 1-year

follow-up ABCD data (95, 97). Each child was asked to make choices between a small immediate hypothetical reward or a larger hypothetical $100 delayed reward at multiple future time points (6h, one day, one week, one month, three months, one year, and five years). By increasing or decreasing the smaller immediate reward depending on the child's response, the task records the indifference point (i.e., the small immediate amount deemed to have the same subjective value as the $100 delayed reward) at each of the seven delay intervals. Test-retest reliability of this delay discounting measure has been validated (98, 99). Studies show that preadolescent children are capable of comprehending the delay discounting task and show similar patterns of discounting as adults (100).

To avoid methodological problems regarding mathematical discounting models (hyperbolic vs. exponential) and positively skewed parameters of discounting functions (99, 101), we used the area under the curve, a model-free measure of delay discounting (101). The area under the curve measure of delay discounting rates (henceforth *discount rates*) ranges from 0 to 1, with lower values indicating steeper discounting and higher impulsivity.

Psychotic-Like Experiences

First and second-year follow-up observations of psychotic-like experiences (PLEs) were measured using the Prodromal Questionnaire-Brief Child Version (PQ-BC; child-reported). PQ-BC has a 21-item scale validated for use with a non-clinical population of children aged 9-10 years (46, 102). In line with the previous research (3, 46, 78, 102), we computed *Total Score* and *Distress Score*, each indicating the number of psychotic-like symptoms and levels of total distress. Total Score is the summary score of 21 questions ranging from 0 to 21, and

Distress Score is the weighted sum of responses with the levels of distress, ranging from 0 to 126. Additionally, to test whether the heterogeneous treatment effects of neighborhood adversity differ among psychotic symptoms, Distress Score was divided into two separate scores: *Delusional Score* and *Hallucinational Score* (2, 103). A higher value indicates greater severity of PLEs.

Genome-wide Polygenic Scores

Children's genetic predisposition were assessed with genome-wide polygenic scores (GPS). Summary statistics from genome-wide association studies were used to generate GPS of cognitive intelligence (cognitive performance (104), education attainment (104), IQ (105)), psychiatric disorders (major depressive disorder(106), post-traumatic stress disorder (107), attention-deficit/hyperactivity disorder(108), obsessive-compulsive disorder (109), anxiety (110), depression (111), bipolar disorder (112), autism spectrum disorder (113), schizophrenia (114), cross disorder (115)), and health and behavioral traits (BMI (116), neuroticism (117), worrying (117), risk tolerance (118), automobile speeding propensity (118), eating disorder (119), drinking(118), smoking (118), cannabis use (120), general happiness (121), snoring (122), insomnia (122), alcohol dependence (123)). PRS-CSx, a high-dimensional Bayesian regression framework that places continuous shrinkage prior on single nucleotide polymorphisms effect sizes (124), was applied to enhance cross-population prediction. This method has consistently shown superior performance compared to other methods across a wide range of genetic architectures in simulation and real data analyses (124). Hyperparameter optimization for the GPSs was conducted using a held-out validation set of

1,579 unrelated participants. Adjustments for population stratification were performed based on the first ten ancestrally informative principal components to account for potential confounding effects.

Anatomical Brain Imaging: T1/T2, Freesurfer 6

Baseline year T1-weighted (T1w) 3D structural MRI acquired in the ABCD study were processed following established protocols (125, 126): To maximize geometric accuracy and image intensity reproducibility, gradient nonlinearity distortion was corrected (127). After correcting intensity nonuniformity using tissue segmentation and spatial smoothing, images were resampled to 1 mm isotropic voxels. We used Freesurfer v6.0 (https://surfer.nmr.mgh.harvard.edu) for the following procedures: cortical surface followed by skull-stripping (128), white matter segmentation, and mesh creation (129), correction of topological defects, surface optimization (130, 131), and nonlinear registration to a spherical surface-based atlas (132). Using Desikan–Killiany atlas (133), a standard atlas for Freesurfer and ABCD study, we extracted 399 brain ROI measures, including volumes, surface area, thickness, mean curvature, sulcal depth, and gyrification.

Functional MRI (fMRI): Monetary Incentive Delay (MID) task

The MID task was used measure the neural activation during anticipation and receipt of monetary gains and losses. In each trial, participants were shown a graphical cue of the 5 possible incentive types: large reward ($5), small reward ($0.20), large loss (-$5), small loss (-$0.20), or neutral ($0). The incentive cue is presented for 2,000 ms, followed by a jittered

anticipatory delay (1,500–4,000 ms). Subsequently, a target to which participants respond to gain or avoid losing money was shown (150–500 ms), and feedback of their performance was provided (2,000 ms). A total of 40 reward, 40 loss, and 20 neutral trials were presented in pseudo-random order across the two task runs. Task parameters was dynamically manipulated for each subject to maintain 60% success rate (126). We used baseline year observations of average beta weights of the MID task fMRI with Desikan-Killiany parcellations (133).

Covariates

To adjust for the potential confounding effects, sociodemographic covariates were included. Consistent with existing research on psychiatric disorders in ABCD samples (3, 46, 78, 134), we controlled for the child's sex, age, race/ethnicity, caregiver's relationship to a child, BMI, parental education, marital status of the caregiver, household income, parent's age, and family history of psychiatric disorders. The family history of psychiatric disorders, measured as the proportion of first-degree relatives who experienced psychosis, depression, mania, suicidality, previous hospitalization, or professional help for mental health issues (3) was included as a covariate. Given that delay discounting and PLEs are associated with an individual's neurocognitive capabilities (135-137), NIH Toolbox total intelligence was used as a covariate. All covariates were from baseline year observations.

Statistical Analyses

Instrumental Variable Regression

The IV method controls unobserved confounding bias by identifying an instrumental variable Z which causally affects the independent variable of interest X but has no direct effect on the dependent variable Y (56). Our instrument variable for ADI was a variable indicating whether the state in each subject resides at baseline year has legislation prohibiting discrimination by the source of income (SOI laws) in the housing market. According to a report by the US Department of Housing and Urban Development, landlords accept housing vouchers 20.2%p~59.3%p higher in local areas with SOI laws (138). Research shows significant reductions in neighborhood poverty rates in locations with SOI laws (139), and those who receive the benefits of housing vouchers in childhood show lower hospitalization rates, less impulsive consumption (140), and substantially better mental health (141). Taken together, we hypothesized that living in states with SOI laws would lead to more moderate discounting of future rewards and fewer PLEs, only through a positive influence on the neighborhood socioeconomic conditions of the subjects.

F-statistic above ten is considered a strong instruments (142). The F-statistic for each model was $F= 35.1423$ ($p<0.0001$), suggesting that our IV model is not likely to suffer from weak instrument bias. Also, testing endogeneity of ADI (i.e., whether ADI as a treatment variable or predictor correlates with the error term), we found that the model was significantly biased by unobserved confounding (all Hausman test (143) for differences, $p<0.0089$). This justifies the need for the IV regression approach to control for the significant confounding effects and to test the causal relationship of neighborhood disadvantage with

delay discounting and psychopathology. All continuous variables were standardized (z-scaled), and analyses were run using *ivreg* (144) in R version 4.1.2. For all analyses, threshold for statistical significance was set at $p<0.05$, with multiple comparison correction based on false discovery rate.

Causal Machine Learning for Treatment Effects

IV Forest (*grf* R package version 2.2.1) (57, 58) is a novel causal machine learning approach extends from the conventional random forest framework (145) with recursive partitioning, subsampling, and random splitting to identify the average treatment effects and its heterogeneity. We obtained augmented inverse propensity weighted estimates of average treatment effects, a doubly-robust estimator which can capture complex patterns of heterogeneity and do not rely on a priori model assumptions (57) such as linearity. This is particularly advantageous when the relationship between environmental variables and neurocognitive development is likely nonlinear (7, 59, 60). To measure the average outcome between treated versus untreated subjects, ADI was binarized (i.e., mean split).

We evaluated heterogeneous treatment effects using the following procedures:

1) Divide the data into 5-folds.

2) Throughout every fold, fit a conditional average treatment effect model on 4 folds, and then rank the unseen observations within the held-out fold into quintiles according to their predicted treatment effects.

3) Obtain augmented inverse propensity weighted average treatment effects for each

quintile.

This is very similar to the generic framework proposed by Chernozhukov, Demirer, Duflo and Fernández-Val (67), which was also used in a recent study (146), except that we used 5-fold cross-validation instead of dividing the data into half for conditional average treatment effect model fitting and ranking observations into subgroups.

Acknowledgements

This work was supported by Institute of Information & communications Technology Planning & Evaluation (IITP) grant funded by the Korea government (MSIT) [NO.2021-0-01343, Artificial Intelligence Graduate School Program (Seoul National University)].

References

1. I. Kant, *Critique of Practical Reason* (Hackett Publishing, 2002).
2. N. R. Karcher, T. A. Niendam, D. M. Barch, Adverse childhood experiences and psychotic-like experiences are associated above and beyond shared correlates: Findings from the adolescent brain cognitive development study. *Schizophrenia Research* **222**, 235-242 (2020).
3. N. R. Karcher, J. Schiffman, D. M. Barch, Environmental Risk Factors and Psychotic-like Experiences in Children Aged 9–10. *Journal of the American Academy of Child & Adolescent Psychiatry* **60**, 490-500 (2021).
4. R. E. Gur *et al.*, Burden of Environmental Adversity Associated With Psychopathology, Maturation, and Brain Behavior Parameters in Youths. *JAMA Psychiatry* **76**, 966 (2019).
5. D. Tomasi, N. D. Volkow, Associations of family income with cognition and brain structure in USA children: prevention implications. *Molecular Psychiatry* 10.1038/s41380-021-01130-0 (2021).
6. T. Vargas, K. S. F. Damme, V. A. Mittal, Neighborhood deprivation, prefrontal morphology and neurocognition in late childhood to early adolescence. *NeuroImage* **220**, 117086 (2020).
7. D. A. Hackman *et al.*, Association of Local Variation in Neighborhood Disadvantage in Metropolitan Areas With Youth Neurocognition and Brain Structure. *JAMA Pediatrics* **175**, e210426 (2021).
8. J. Ye *et al.*, Socioeconomic Deprivation Index Is Associated With Psychiatric Disorders: An Observational and Genome-wide Gene-by-Environment Interaction Analysis in the UK Biobank Cohort. *Biol Psychiatry* **89**, 888-895 (2021).
9. J. Bor, G. H. Cohen, S. Galea, Population health in an era of rising income inequality: USA, 1980–2015. *The Lancet* **389**, 1475-1490 (2017).
10. E. Dennis, P. Manza, N. D. Volkow, Socioeconomic status, BMI, and brain development in children. *Transl Psychiatry* **12** (2022).
11. T. Leventhal, J. Brooks-Gunn, The neighborhoods they live in: The effects of neighborhood residence on child and adolescent outcomes. *Psychological Bulletin* **126**, 309-337 (2000).
12. T. Leventhal, J. Brooks-Gunn, A Randomized Study of Neighborhood Effects on Low Income Children's Educational Outcomes. *Developmental Psychology* **40**, 488-507 (2004).
13. P. Oreopoulos, The Long-Run Consequences of Living in a Poor Neighborhood*. *The Quarterly Journal of Economics* **118**, 1533-1575 (2003).
14. F. Campbell *et al.*, Early Childhood Investments Substantially Boost Adult Health. *Science* **343**, 1478-1485 (2014).
15. J. J. Heckman, J. Stixrud, S. Urzua, The effects of cognitive and noncognitive abilities on labor market outcomes and social behavior. *Journal of Labor Economics* **24**, 411-482 (2006).
16. E. I. Knudsen, J. J. Heckman, J. L. Cameron, J. P. Shonkoff, Economic, neurobiological, and behavioral perspectives on building America's future workforce. *Proceedings of the National Academy of Sciences* **103**, 10155-10162 (2006).
17. R. Chetty, N. Hendren, The Impacts of Neighborhoods on Intergenerational Mobility I: Childhood Exposure Effects*. *The Quarterly Journal of Economics* **133**, 1107-1162 (2018).
18. R. Chetty, N. Hendren, L. F. Katz, The Effects of Exposure to Better Neighborhoods on Children: New Evidence from the Moving to Opportunity Experiment. *Am Econ Rev* **106**, 855-902 (2016).
19. R. G. Fryer, L. F. Katz, Achieving Escape Velocity: Neighborhood and School Interventions to Reduce Persistent Inequality. *Am Econ Rev* **103**, 232-237 (2013).
20. J. J. Heckman, Skill Formation and the Economics of Investing in Disadvantaged Children. *Science* **312**, 1900-1902 (2006).
21. C. J. Lowe, J. B. Morton, A. C. Reichelt, Adolescent Obesity and Dietary Decision Making—

a Brain-Health Perspective. *The Lancet Child & Adolescent Health* **4**, 388-396 (2020).
22. J. P. Shonkoff, Leveraging the biology of adversity to address the roots of disparities in health and development. *Proceedings of the National Academy of Sciences* **109**, 17302-17307 (2012).
23. J. P. Shonkoff, Capitalizing on Advances in Science to Reduce the Health Consequences of Early Childhood Adversity. *JAMA Pediatrics* **170**, 1003 (2016).
24. H. Zhang, Z. X. Lee, T. White, A. Qiu, Parental and social factors in relation to child psychopathology, behavior, and cognitive function. *Transl Psychiatry* **10** (2020).
25. P. Pechtel, D. A. Pizzagalli, Disrupted Reinforcement Learning and Maladaptive Behavior in Women With a History of Childhood Sexual Abuse. *JAMA Psychiatry* **70**, 499 (2013).
26. A. Oshri *et al.*, Socioeconomic hardship and delayed reward discounting: Associations with working memory and emotional reactivity. *Developmental Cognitive Neuroscience* **37**, 100642 (2019).
27. J. Kim□Spoon *et al.*, Longitudinal pathways linking family risk, neural risk processing, delay discounting, and adolescent substance use. *Journal of Child Psychology and Psychiatry* **60**, 655-664 (2019).
28. J. Park *et al.*, Gene-Environment Causal Pathway to Impoverished Cognitive Development Contributes to Psychotic-Like Experience in Children. *medRxiv* 10.1101/2021.12.28.21268440, 2021.2012.2028.21268440 (2021).
29. Z. A. Yaple, R. Yu, Functional and Structural Brain Correlates of Socioeconomic Status. *Cerebral Cortex* **30**, 181-196 (2020).
30. T. Epper *et al.*, Time Discounting and Wealth Inequality. *Am Econ Rev* **110**, 1177-1205 (2020).
31. T. Epper *et al.*, Preferences predict who commits crime among young men. *Proceedings of the National Academy of Sciences* **119**, e2112645119 (2022).
32. K. M. Ericson, D. Laibson, "Intertemporal choice" in Handbook of Behavioral Economics: Applications and Foundations 1, B. D. Bernheim, S. DellaVigna, D. Laibson, Eds. (North-Holland, 2019), vol. 2, chap. Chapter 1, pp. 1-67.
33. R. Laajaj, Endogenous time horizon and behavioral poverty trap: Theory and evidence from Mozambique. *Journal of Development Economics* **127**, 187-208 (2017).
34. T. V. Maia, M. J. Frank, From reinforcement learning models to psychiatric and neurological disorders. *Nature Neuroscience* **14**, 154-162 (2011).
35. K. Juechems, C. Summerfield, Where Does Value Come From? *Trends in Cognitive Sciences* **23**, 836-850 (2019).
36. T. V. Maia, M. J. Frank, An Integrative Perspective on the Role of Dopamine in Schizophrenia. *Biol Psychiatry* **81**, 52-66 (2017).
37. S. J. Millard, C. E. Bearden, K. H. Karlsgodt, M. J. Sharpe, The prediction-error hypothesis of schizophrenia: new data point to circuit-specific changes in dopamine activity. *Neuropsychopharmacology* **47**, 628-640 (2022).
38. D. H. Zald, M. T. Treadway, Reward Processing, Neuroeconomics, and Psychopathology. *Annu Rev Clin Psychol* **13**, 471-495 (2017).
39. W.-Y. Ahn *et al.*, Temporal discounting of rewards in patients with bipolar disorder and schizophrenia. *Journal of Abnormal Psychology* **120**, 911-921 (2011).
40. A. O. Ermakova *et al.*, Abnormal reward prediction-error signalling in antipsychotic naive individuals with first-episode psychosis or clinical risk for psychosis. *Neuropsychopharmacology* **43**, 1691-1699 (2018).
41. M. Amlung *et al.*, Delay Discounting as a Transdiagnostic Process in Psychiatric Disorders. *JAMA Psychiatry* **76**, 1176 (2019).
42. A. M. Gard *et al.*, Beyond family□level adversities: Exploring the developmental timing of neighborhood disadvantage effects on the brain. *Developmental Science* **24** (2021).
43. D. Rakesh, C. Seguin, A. Zalesky, V. Cropley, S. Whittle, Associations between neighborhood disadvantage, resting-state functional connectivity, and behavior in the Adolescent Brain

Cognitive Development (ABCD) Study®: Moderating role of positive family and school environments. *Biological Psychiatry: Cognitive Neuroscience and Neuroimaging* https://doi.org/10.1016/j.bpsc.2021.03.008 (2021).

44. R. L. Taylor, S. R. Cooper, J. J. Jackson, D. M. Barch, Assessment of Neighborhood Poverty, Cognitive Function, and Prefrontal and Hippocampal Volumes in Children. *JAMA Network Open* **3**, e2023774 (2020).
45. J. Newbury *et al.*, Cumulative Effects of Neighborhood Social Adversity and Personal Crime Victimization on Adolescent Psychotic Experiences. *Schizophrenia Bulletin* **44**, 348-358 (2018).
46. N. R. Karcher *et al.*, Assessment of the Prodromal Questionnaire–Brief Child Version for Measurement of Self-reported Psychotic-like Experiences in Childhood. *JAMA Psychiatry* **75**, 853 (2018).
47. E. M. Derks, J. G. Thorp, Z. F. Gerring, Ten challenges for clinical translation in psychiatric genetics. *Nature Genetics* **54**, 1457-1465 (2022).
48. S. Kapur, A. G. Phillips, T. R. Insel, Why has it taken so long for biological psychiatry to develop clinical tests and what to do about it? *Molecular Psychiatry* **17**, 1174-1179 (2012).
49. S. Sanchez-Roige *et al.*, Genome-wide association study of delay discounting in 23,217 adult research participants of European ancestry. *Nature Neuroscience* **21**, 16-18 (2018).
50. M. M. Owens *et al.*, Functional and structural neuroimaging studies of delayed reward discounting in addiction: A systematic review. *Psychological Bulletin* **145**, 141-164 (2019).
51. M. A. Hamburg, F. S. Collins, The Path to Personalized Medicine. *New England Journal of Medicine* **363**, 301-304 (2010).
52. D. M. Kent *et al.*, The Predictive Approaches to Treatment effect Heterogeneity (PATH) Statement. *Annals of Internal Medicine* **172**, 35-45 (2019).
53. R. Border *et al.*, No Support for Historical Candidate Gene or Candidate Gene-by-Interaction Hypotheses for Major Depression Across Multiple Large Samples. *American Journal of Psychiatry* **176**, 376-387 (2019).
54. D. N. Figlio, J. Freese, K. Karbownik, J. Roth, Socioeconomic status and genetic influences on cognitive development. *Proceedings of the National Academy of Sciences* **114**, 13441-13446 (2017).
55. E. T. Akimova, R. Breen, D. M. Brazel, M. C. Mills, Gene-environment dependencies lead to collider bias in models with polygenic scores. *Scientific Reports* **11** (2021).
56. J. D. Angrist, G. W. Imbens, D. B. Rubin, Identification of Causal Effects Using Instrumental Variables. *Journal of the American Statistical Association* **91**, 444-455 (1996).
57. S. Athey, J. Tibshirani, S. Wager, Generalized random forests. *The Annals of Statistics* **47**, 1148-1178 (2019).
58. S. Wager, S. Athey, Estimation and Inference of Heterogeneous Treatment Effects using Random Forests. *Journal of the American Statistical Association* **113**, 1228-1242 (2018).
59. M. G. Berman, A. J. Stier, G. N. Akcelik, Environmental neuroscience. *Am Psychol* **74**, 1039-1052 (2019).
60. U. A. Tooley, D. S. Bassett, A. P. Mackey, Environmental influences on the pace of brain development. *Nature Reviews Neuroscience* **22**, 372-384 (2021).
61. P. Bach, V. Chernozhukov, M. S. Kurz, M. Spindler, DoubleML-An Object-Oriented Implementation of Double Machine Learning in Python. *Journal of Machine Learning Research* **23**, 1-6 (2022).
62. V. Chernozhukov *et al.*, Double/debiased machine learning for treatment and structural parameters. *The Econometrics Journal* **21**, C1-C68 (2018).
63. M. B. Kursa, W. R. Rudnicki, Feature Selection with the Boruta Package. *Journal of Statistical Software* **36**, 1 - 13 (2010).
64. G. Sveinbjornsson *et al.*, Multiomics study of nonalcoholic fatty liver disease. *Nature*

Genetics **54**, 1652-1663 (2022).

65. Z. Wang, X. Zhou, Y. Gui, M. Liu, H. Lu, Multiple measurement analysis of resting-state fMRI for ADHD classification in adolescent brain from the ABCD study. *Transl Psychiatry* **13**, 45 (2023).
66. G. Ball *et al.*, Machine-learning to characterise neonatal functional connectivity in the preterm brain. *NeuroImage* **124**, 267-275 (2016).
67. V. Chernozhukov, M. Demirer, E. Duflo, I. Fernández-Val, Generic Machine Learning Inference on Heterogeneous Treatment Effects in Randomized Experiments, with an Application to Immunization in India. *National Bureau of Economic Research Working Paper Series* **No. 24678** (2018).
68. S. M. Lundberg *et al.*, From local explanations to global understanding with explainable AI for trees. *Nature Machine Intelligence* **2**, 56-67 (2020).
69. D. Tingley, T. Yamamoto, K. Hirose, L. Keele, K. Imai, mediation: R package for causal mediation analysis. *Journal of Statistical Software* **59** (2014).
70. G. S. Becker, C. B. Mulligan, The Endogenous Determination of Time Preference. *The Quarterly Journal of Economics* **112**, 729-758 (1997).
71. F. Cunha, J. J. Heckman, The Economics and Psychology of Inequality and Human Development. *Journal of the European Economic Association* **7**, 320-364 (2009).
72. M. Niwa *et al.*, Adolescent Stress–Induced Epigenetic Control of Dopaminergic Neurons via Glucocorticoids. *Science* **339**, 335-339 (2013).
73. R. M. Birn, B. J. Roeber, S. D. Pollak, Early childhood stress exposure, reward pathways, and adult decision making. *Proceedings of the National Academy of Sciences* **114**, 13549-13554 (2017).
74. P. DeRosse, A. D. Barber, Overlapping Neurobiological Substrates for Early-Life Stress and Resilience to Psychosis. *Biological Psychiatry: Cognitive Neuroscience and Neuroimaging* **6**, 144-153 (2021).
75. P. Shaw *et al.*, Neurodevelopmental Trajectories of the Human Cerebral Cortex. *The Journal of Neuroscience* **28**, 3586 (2008).
76. L. M. Reynolds, C. Flores, Mesocorticolimbic Dopamine Pathways Across Adolescence: Diversity in Development. *Frontiers in Neural Circuits* **15** (2021).
77. D. E. Vosberg, M. Leyton, C. Flores, The Netrin-1/DCC guidance system: dopamine pathway maturation and psychiatric disorders emerging in adolescence. *Molecular Psychiatry* **25**, 297-307 (2020).
78. N. R. Karcher *et al.*, Psychotic-like Experiences and Polygenic Liability in the Adolescent Brain Cognitive Development Study. *Biological Psychiatry: Cognitive Neuroscience and Neuroimaging* https://doi.org/10.1016/j.bpsc.2021.06.012 (2021).
79. L. Hubbard *et al.*, Evidence of Common Genetic Overlap Between Schizophrenia and Cognition. *Schizophrenia Bulletin* **42**, 832-842 (2016).
80. U. Bronfenbrenner, S. J. Ceci, Nature-nuture reconceptualized in developmental perspective: A bioecological model. *Psychological Review* **101**, 568-586 (1994).
81. J. Gottschling *et al.*, Socioeconomic status amplifies genetic effects in middle childhood in a large German twin sample. *Intelligence* **72**, 20-27 (2019).
82. E. Turkheimer, A. Haley, M. Waldron, B. D'Onofrio, I. I. Gottesman, Socioeconomic Status Modifies Heritability of IQ in Young Children. *Psychol Sci* **14**, 623-628 (2003).
83. R. Lewontin, *Human Diversity* (Scientific American Library, New York, 1995).
84. H.-H. Wang *et al.*, The Impact of Early Life Stress on the Genetic Influence on Brain and Cognitive Development in Children. *medRxiv* 10.1101/2021.12.27.21268445, 2021.2012.2027.21268445 (2021).
85. M. J. Taylor, D. Freeman, S. Lundström, H. Larsson, A. Ronald, Heritability of Psychotic Experiences in Adolescents and Interaction With Environmental Risk. *JAMA Psychiatry* **79**,

889 (2022).

86. S. C. South, R. F. Krueger, Genetic and environmental influences on internalizing psychopathology vary as a function of economic status. *Psychological Medicine* **41**, 107-117 (2011).
87. T. C. Bates, G. J. Lewis, A. Weiss, Childhood Socioeconomic Status Amplifies Genetic Effects on Adult Intelligence. *Psychol Sci* **24**, 2111-2116 (2013).
88. P. A. Demange *et al.*, Investigating the genetic architecture of noncognitive skills using GWAS-by-subtraction. *Nature Genetics* **53**, 35-44 (2021).
89. D. W. Belsky *et al.*, Genetic analysis of social-class mobility in five longitudinal studies. *Proceedings of the National Academy of Sciences* **115**, E7275-E7284 (2018).
90. D. Barth, N. W. Papageorge, K. Thom, Genetic endowments and wealth inequality. *Journal of Political Economy* **128**, 1474-1522 (2020).
91. D. M. Kent, E. Steyerberg, D. van Klaveren, Personalized evidence based medicine: predictive approaches to heterogeneous treatment effects. *BMJ* **363**, k4245 (2018).
92. K. Ruggeri *et al.*, The globalizability of temporal discounting. *Nature Human Behaviour* 10.1038/s41562-022-01392-w (2022).
93. R. Poulton *et al.*, Children's Self-Reported Psychotic Symptoms and Adult Schizophreniform Disorder. *Archives of General Psychiatry* **57**, 1053 (2000).
94. N. R. Karcher, D. M. Barch, The ABCD study: understanding the development of risk for mental and physical health outcomes. *Neuropsychopharmacology* **46**, 131-142 (2021).
95. M. Luciana *et al.*, Adolescent neurocognitive development and impacts of substance use: Overview of the adolescent brain cognitive development (ABCD) baseline neurocognition battery. *Developmental Cognitive Neuroscience* **32**, 67-79 (2018).
96. M. W. Johnson, W. K. Bickel, An algorithm for identifying nonsystematic delay-discounting data. *Experimental and Clinical Psychopharmacology* **16**, 264-274 (2008).
97. M. N. Koffarnus, W. K. Bickel, A 5-trial adjusting delay discounting task: Accurate discount rates in less than one minute. *Experimental and Clinical Psychopharmacology* **22**, 222-228 (2014).
98. A. K. Matusiewicz, A. E. Carter, R. D. Landes, R. Yi, Statistical equivalence and test–retest reliability of delay and probability discounting using real and hypothetical rewards. *Behavioural Processes* **100**, 116-122 (2013).
99. M. M. Owens *et al.*, One-year predictions of delayed reward discounting in the adolescent brain cognitive development study. *Experimental and Clinical Psychopharmacology* 10.1037/pha0000532, No Pagination Specified-No Pagination Specified (2021).
100. P. Burns *et al.*, Examining children's ability to delay reward: Is the delay discounting task a suitable measure? *Journal of Behavioral Decision Making* **33**, 208-219 (2020).
101. J. Myerson, L. Green, M. Warusawitharana, AREA UNDER THE CURVE AS A MEASURE OF DISCOUNTING. *Journal of the Experimental Analysis of Behavior* **76**, 235-243 (2001).
102. N. R. Karcher, M. T. Perino, D. M. Barch, An item response theory analysis of the Prodromal Questionnaire-Brief Child Version: Developing a screening form that informs understanding of self-reported psychotic-like experiences in childhood. *Journal of Abnormal Psychology* **129**, 293-304 (2020).
103. N. R. Karcher, K. J. O'Brien, S. Kandala, D. M. Barch, Resting-State Functional Connectivity and Psychotic-like Experiences in Childhood: Results From the Adolescent Brain Cognitive Development Study. *Biol Psychiatry* **86**, 7-15 (2019).
104. J. J. Lee *et al.*, Gene discovery and polygenic prediction from a genome-wide association study of educational attainment in 1.1 million individuals. *Nature Genetics* **50**, 1112-1121 (2018).
105. J. E. Savage *et al.*, Genome-wide association meta-analysis in 269,867 individuals identifies new genetic and functional links to intelligence. *Nature Genetics* **50**, 912-919 (2018).

106. N. R. Wray *et al.*, Genome-wide association analyses identify 44 risk variants and refine the genetic architecture of major depression. *Nature Genetics* **50**, 668-681 (2018).
107. C. M. Nievergelt *et al.*, International meta-analysis of PTSD genome-wide association studies identifies sex- and ancestry-specific genetic risk loci. *Nature Communications* **10**, 4558 (2019).
108. D. Demontis *et al.*, Discovery of the first genome-wide significant risk loci for attention deficit/hyperactivity disorder. *Nature Genetics* **51**, 63-75 (2019).
109. P. D. Arnold *et al.*, Revealing the complex genetic architecture of obsessive–compulsive disorder using meta-analysis. *Molecular Psychiatry* **23**, 1181-1188 (2018).
110. T. Otowa *et al.*, Meta-analysis of genome-wide association studies of anxiety disorders. *Molecular Psychiatry* **21**, 1391-1399 (2016).
111. D. M. Howard *et al.*, Genome-wide meta-analysis of depression identifies 102 independent variants and highlights the importance of the prefrontal brain regions. *Nature Neuroscience* **22**, 343-352 (2019).
112. E. A. Stahl *et al.*, Genome-wide association study identifies 30 loci associated with bipolar disorder. *Nature Genetics* **51**, 793-803 (2019).
113. J. Grove *et al.*, Identification of common genetic risk variants for autism spectrum disorder. *Nature Genetics* **51**, 431-444 (2019).
114. D. M. Ruderfer *et al.*, Genomic Dissection of Bipolar Disorder and Schizophrenia, Including 28 Subphenotypes. *Cell* **173**, 1705-1715.e1716 (2018).
115. Anonymous, Identification of risk loci with shared effects on five major psychiatric disorders: a genome-wide analysis. *The Lancet* **381**, 1371-1379 (2013).
116. A. E. Locke *et al.*, Genetic studies of body mass index yield new insights for obesity biology. *Nature* **518**, 197-206 (2015).
117. M. Nagel *et al.*, Meta-analysis of genome-wide association studies for neuroticism in 449,484 individuals identifies novel genetic loci and pathways. *Nature Genetics* **50**, 920-927 (2018).
118. R. Karlsson Linnér *et al.*, Genome-wide association analyses of risk tolerance and risky behaviors in over 1 million individuals identify hundreds of loci and shared genetic influences. *Nature Genetics* **51**, 245-257 (2019).
119. H. J. Watson *et al.*, Genome-wide association study identifies eight risk loci and implicates metabo-psychiatric origins for anorexia nervosa. *Nature Genetics* **51**, 1207-1214 (2019).
120. J. A. Pasman *et al.*, GWAS of lifetime cannabis use reveals new risk loci, genetic overlap with psychiatric traits, and a causal effect of schizophrenia liability. *Nature Neuroscience* **21**, 1161-1170 (2018).
121. A. Okbay *et al.*, Genetic variants associated with subjective well-being, depressive symptoms, and neuroticism identified through genome-wide analyses. *Nature Genetics* **48**, 624-633 (2016).
122. P. R. Jansen *et al.*, Genome-wide analysis of insomnia in 1,331,010 individuals identifies new risk loci and functional pathways. *Nature Genetics* **51**, 394-403 (2019).
123. R. K. Walters *et al.*, Transancestral GWAS of alcohol dependence reveals common genetic underpinnings with psychiatric disorders. *Nature Neuroscience* **21**, 1656-1669 (2018).
124. T. Ge, C.-Y. Chen, Y. Ni, Y.-C. A. Feng, J. W. Smoller, Polygenic prediction via Bayesian regression and continuous shrinkage priors. *Nature Communications* **10** (2019).
125. H. Garavan *et al.*, Recruiting the ABCD sample: Design considerations and procedures. *Developmental Cognitive Neuroscience* **32**, 16-22 (2018).
126. B. J. Casey *et al.*, The Adolescent Brain Cognitive Development (ABCD) study: Imaging acquisition across 21 sites. *Developmental Cognitive Neuroscience* **32**, 43-54 (2018).
127. J. Jovicich *et al.*, Reliability in multi-site structural MRI studies: Effects of gradient non-linearity correction on phantom and human data. *NeuroImage* **30**, 436-443 (2006).
128. F. Ségonne *et al.*, A hybrid approach to the skull stripping problem in MRI. *NeuroImage* **22**,

1060-1075 (2004).

129. A. M. Dale, B. Fischl, M. I. Sereno, Cortical Surface-Based Analysis: I. Segmentation and Surface Reconstruction. *NeuroImage* **9**, 179-194 (1999).
130. B. Fischl, A. Liu, A. M. Dale, Automated manifold surgery: constructing geometrically accurate and topologically correct models of the human cerebral cortex. *IEEE Transactions on Medical Imaging* **20**, 70-80 (2001).
131. F. Segonne, J. Pacheco, B. Fischl, Geometrically Accurate Topology-Correction of Cortical Surfaces Using Nonseparating Loops. *IEEE Transactions on Medical Imaging* **26**, 518-529 (2007).
132. B. Fischl, M. I. Sereno, R. B. H. Tootell, A. M. Dale, High-resolution intersubject averaging and a coordinate system for the cortical surface. *Human Brain Mapping* **8**, 272-284 (1999).
133. R. S. Desikan *et al.*, An automated labeling system for subdividing the human cerebral cortex on MRI scans into gyral based regions of interest. *NeuroImage* **31**, 968-980 (2006).
134. M. T. van Dijk, E. Murphy, J. E. Posner, A. Talati, M. M. Weissman, Association of Multigenerational Family History of Depression With Lifetime Depressive and Other Psychiatric Disorders in Children. *JAMA Psychiatry* 10.1001/jamapsychiatry.2021.0350 (2021).
135. A. P. Anokhin, J. D. Grant, R. C. Mulligan, A. C. Heath, The Genetics of Impulsivity: Evidence for the Heritability of Delay Discounting. *Biol Psychiatry* **77**, 887-894 (2015).
136. N. A. Shamosh, J. R. Gray, Delay discounting and intelligence: A meta-analysis. *Intelligence* **36**, 289-305 (2008).
137. K. Keidel, Q. Rramani, B. Weber, C. Murawski, U. Ettinger, Individual Differences in Intertemporal Choice. *Frontiers in Psychology* **12** (2021).
138. M. Cunningham *et al.* (2018) A Pilot Study of Landlord Acceptance of Housing Choice Vouchers. (US Department of Housing and Urban Development, Office of Policy Development and Research, Washington, DC).
139. L. Freeman, Y. Li, Do Source of Income Anti-discrimination Laws Facilitate Access to Less Disadvantaged Neighborhoods? *Housing Studies* **29**, 88-107 (2014).
140. C. E. Pollack *et al.*, Association of Receipt of a Housing Voucher With Subsequent Hospital Utilization and Spending. *JAMA* **322**, 2115-2124 (2019).
141. J. R. Kling, J. B. Liebman, L. F. Katz, Experimental Analysis of Neighborhood Effects. *Econometrica* **75**, 83-119 (2007).
142. D. Staiger, J. H. Stock, Instrumental Variables Regression with Weak Instruments. *Econometrica* **65**, 557 (1997).
143. J. A. Hausman, Specification Tests in Econometrics. *Econometrica* **46**, 1251 (1978).
144. J. Fox, C. Kleiber, A. Zeileis, N. Kuschnig (2021) ivreg: Instrumental-Variables Regression by '2SLS', '2SM', or '2SMM', with Diagnostics. pp Instrumental variable estimation for linear models by two-stage least-squares (2SLS) regression or by robust-regression via M-estimation (2SM) or MMestimation (2SMM). The main ivreg() model-fitting function is designed to provide a workflow as similar as possible to standard lm() regression. A wide range of methods is provided for fitted ivreg model objects, including extensive functionality for computing and graphing regression diagnostics in addition to other standard model tools.
145. L. Breiman, Random Forests. *Machine Learning* **45**, 5-32 (2001).
146. E. C. Goligher *et al.*, Heterogeneous Treatment Effects of Therapeutic-Dose Heparin in Patients Hospitalized for COVID-19. *JAMA* 10.1001/jama.2023.3651 (2023).

Figures and Tables

Figure 1. Heterogeneous treatment effects of neighborhood socioeconomic adversity on psychotic risk. Subjects were divided into quintiles by their relative resilience/vulnerability to the impact of neighborhood deprivation on PLEs (Q1: most resilient~Q5: most vulnerable). Average values of conditional average treatment effects (CATE) within more vulnerable subgroups were significantly different from that of the most resilient subgroup (Q1). Statistical significance is marked with stars (*: p-FDR<0.05, **: p-FDR<0.005, ***: p-FDR<0.0005).

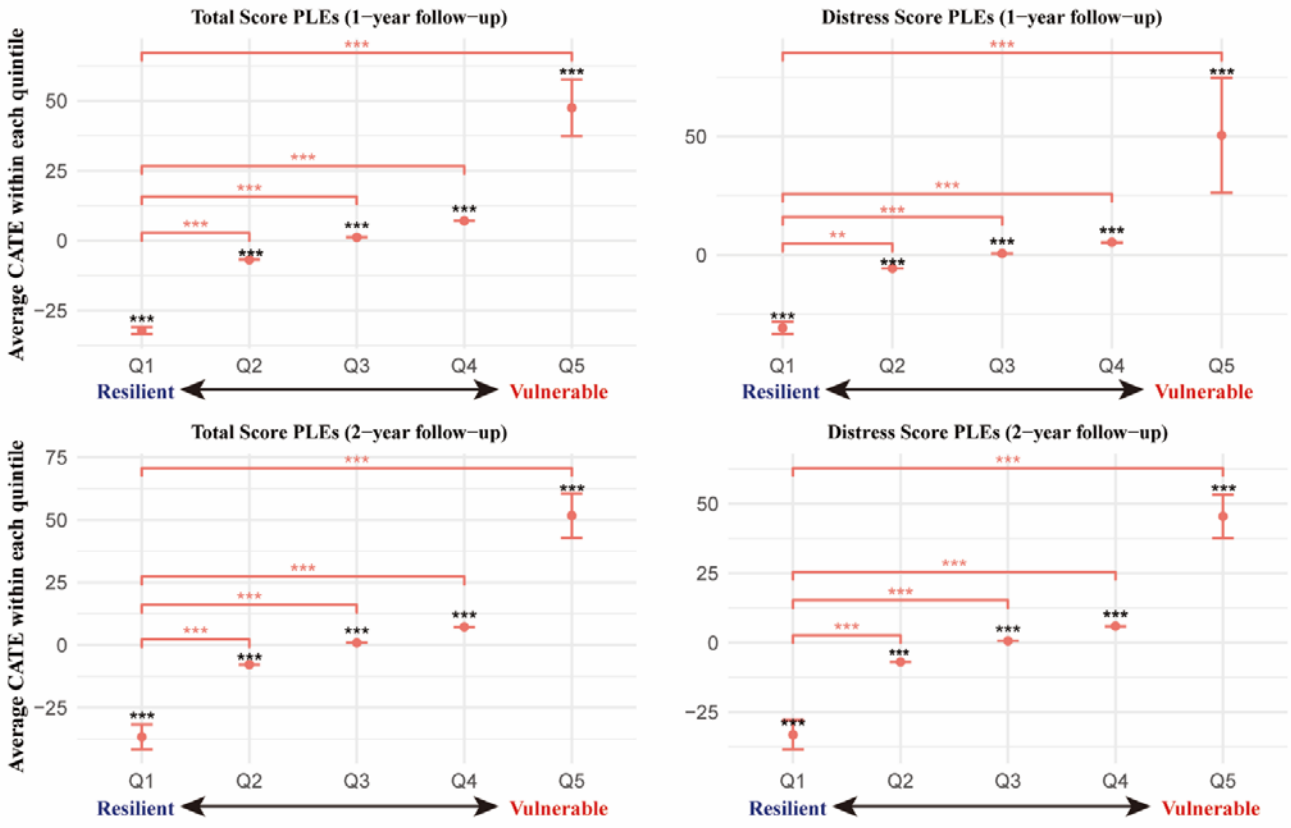

Figure 2. Beeswarm summary plots of Shapley additive explanation (SHAP) values for IV Forest models. Contributions of the top 20 variables of highest importance in the IV Forest model for the heterogeneous treatment effects of neighborhood deprivation are shown. Variables are ordered by their relative importance in the model. Positive SHAP values indicate greater vulnerability (lower resilience) to the effects of ADI on PLEs; negative values indicate lower vulnerability (greater resilience). Contrasts of average beta activations of the given brain ROIs during MID tasks are shown in parenthesis. R vs N denote contrasts between any rewards and neutral reward, L vs N, contrasts between any loss and neutral reward. Ventral dc: ventral diencephalon.

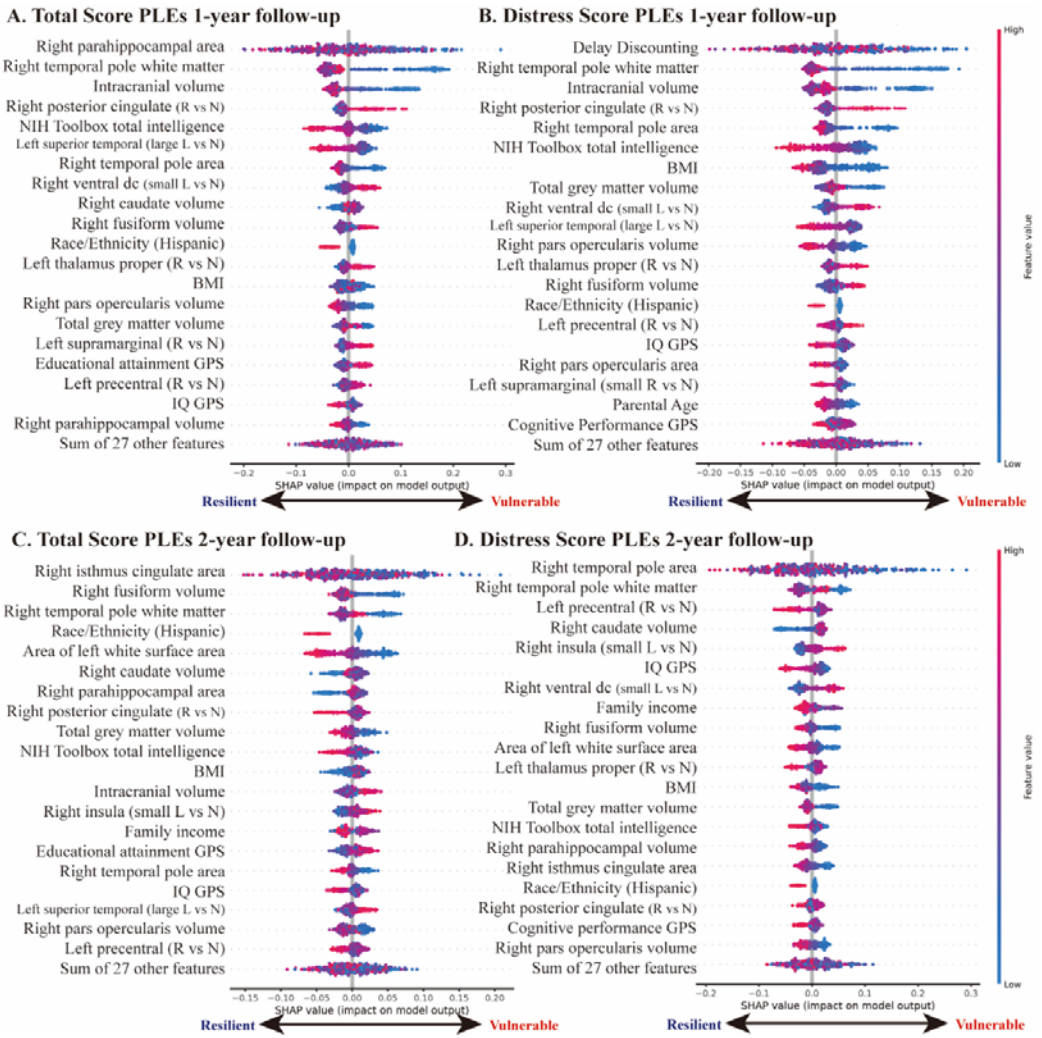

Figure 3. Additional analyses for the heterogeneous effects of neighborhood deprivation. (A) Reduced model with GPS and brain ROIs jointly associated with both delay discounting and PLEs. In the reduced model, the effects of neighborhood deprivation on 1-year follow-up Total Score PLEs within more vulnerable subgroups (Q2~Q4) were not significantly from that of the most resilient group (Q1). (B) Symptom-specific analysis with Delusional Score and Hallucinational Score PLEs. For both symptoms, the differential effects of neighborhood deprivation were significant. Statistical significance is marked with stars (*: p-FDR<0.05, **: p-FDR<0.005, ***: p-FDR<0.0005). CATE: conditional average treatment effects.

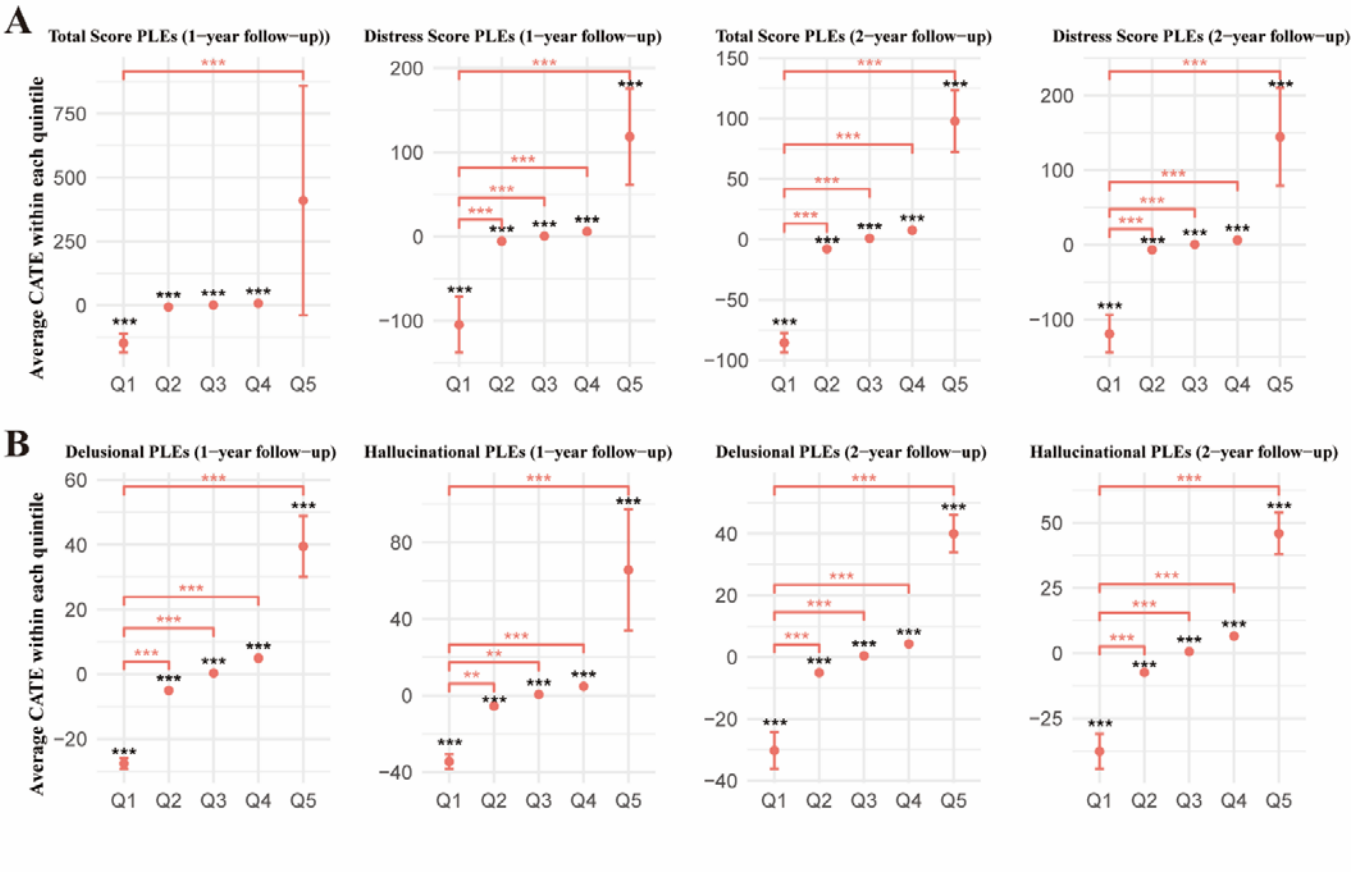

Figure 4. Beeswarm summary plots of SHAP values of IV Forest models with symptom specific PLEs. Contributions of the top 20 variables of highest importance in the IV Forest model for the heterogeneous treatment effects of neighborhood deprivation are shown. Variables are ordered by their relative importance in the model. Positive SHAP values indicate greater vulnerability (lower resilience) to the effects of ADI on PLEs; negative values indicate lower vulnerability (greater resilience). Contrasts of average beta activations of the given brain ROIs during MID tasks are shown in parenthesis. R vs N denote contrasts between any rewards and neutral reward, L vs N, contrasts between any loss and neutral reward. Ventral dc: ventral diencephalon.

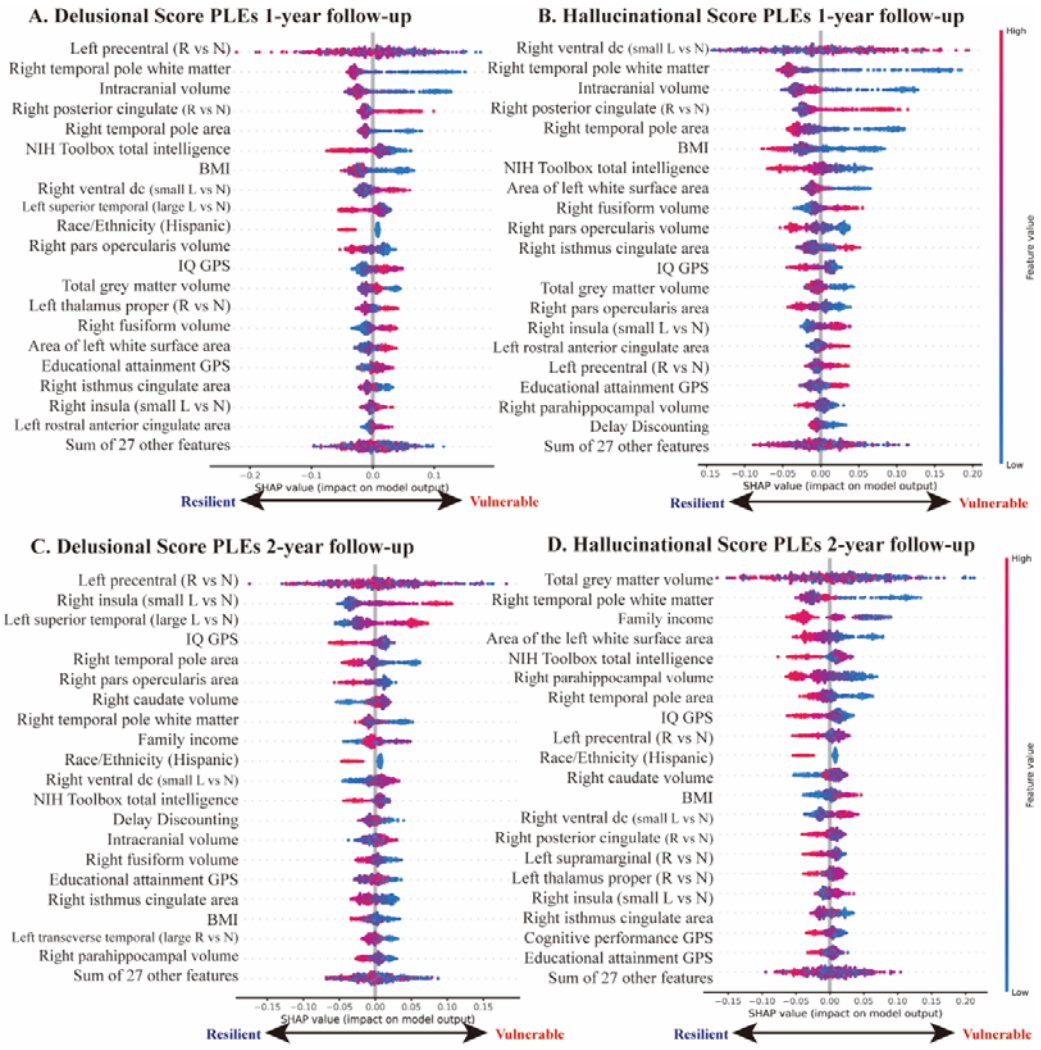

Table 1. Socioeconomic/demographic characteristics of the participants. *Age* is rounded to chronological month. *Parental Education* is measured as the highest grade or level of school completed or highest degree received. *Family History of Psychiatric Disorders* represents the proportion of first-degree relatives who experienced mental illness.

Demographic Characteristics		N	Ratio (%)	Mean (SD)
Age		2,135		120.1541 (7.4658)
Sex	Male	1,517	53.86%	
	Female	985	46.14%	
Marital Status of the first caregiver	Married	1,636	76.63%	
	Widowed	12	0.56%	
	Divorced	193	9.04%	
	Separated	62	2.9%	
	Never Married	142	6.65%	

	Living with Partner	90	4.22%	
Race/Ethnicity	White	1,400	65.57%	
	Black	136	6.37%	
	Hispanic	373	17.47%	
	Asian	7	0.33%	
	Other	219	10.26%	
Parent's Identity	Biological Mother	1,848	86.56%	
	Biological Father	215	10.07%	
	Adoptive Parent	39	1.83%	
	Custodial Parent	12	0.56%	
	Other	21	0.98%	
Household Income		2,135		$70,245 (1.937)
Parental Education		2,135		17.2838 (2.3046)
BMI		2,135		18.4298 (3.8572)

Parental Age		2,135		40.8775 (6.3825)
Family History of Psychiatric Disorders		2,135		0.0958 (0.1125)

Table 2. Causal effects of neighborhood socioeconomic adversity on intertemporal valuation and psychotic risk. Average treatment effects of ADI on delay discounting and PLEs in the IV Forest models are shown. All p-values were corrected for multiple comparison using false discovery rate.

	IV Forests: Average Treatment Effects				
	Estimates	**Std. Error**	**95% Lower CI**	**95% Upper CI**	**P-FDR**
Discount Rate (1-year follow-up)	-1.7297	0.7475	-3.1948	-0.2645	0.0258
Total Score PLE (1-year follow-up)	1.528	0.6432	0.2673	2.7886	0.0258
Distress Score PLE (1-year follow-up)	1.8721	0.6118	0.6729	3.0712	0.0111
Total Score PLE (2-year follow-up)	1.3425	0.6152	0.1367	2.5483	0.0291
Distress Score PLE (2-year follow-up)	1.5042	0.5917	0.3445	2.6638	0.0258

Supporting Information for

Heterogeneity in the Effects of Neighborhood Deprivation on Economic Decision Making and Mental Health in Children

Junghoon Park, Minje Cho, Eunji Lee, Bo-Gyeom Kim, Gakyung Kim, Yoonjung Yoonie Joo, Jiook Cha*

*Corresponding Author: Jiook Cha, PhD

Email: connectome@snu.ac.kr

This PDF file includes:

Supporting text

Figures S1

Tables S1 to S8

SI References

SI Appendix

Fig. S1. Beeswarm summary plots of SHAP values of all covariates. (A) Total Score PLEs 1-year follow-up. (B) Distress Score PLEs 1-year follow-up. (C) Total Score PLEs 2-year follow-up. (D) Distress Score PLEs 2-year follow-up. Contributions of all covariates in the IV Forest model for the heterogeneous treatment effects of neighborhood deprivation are shown. Variables are ordered by their relative importance in the model. Positive SHAP values indicate greater vulnerability (lower resilience) to the effects of ADI on PLEs; negative values indicate lower vulnerability (greater resilience). Contrasts of average beta activations of the given brain ROIs during MID tasks are shown in parenthesis. R vs N denote contrasts between any rewards and neutral reward, L vs N, contrasts between any loss and neutral reward. Ventral dc: ventral diencephalon.

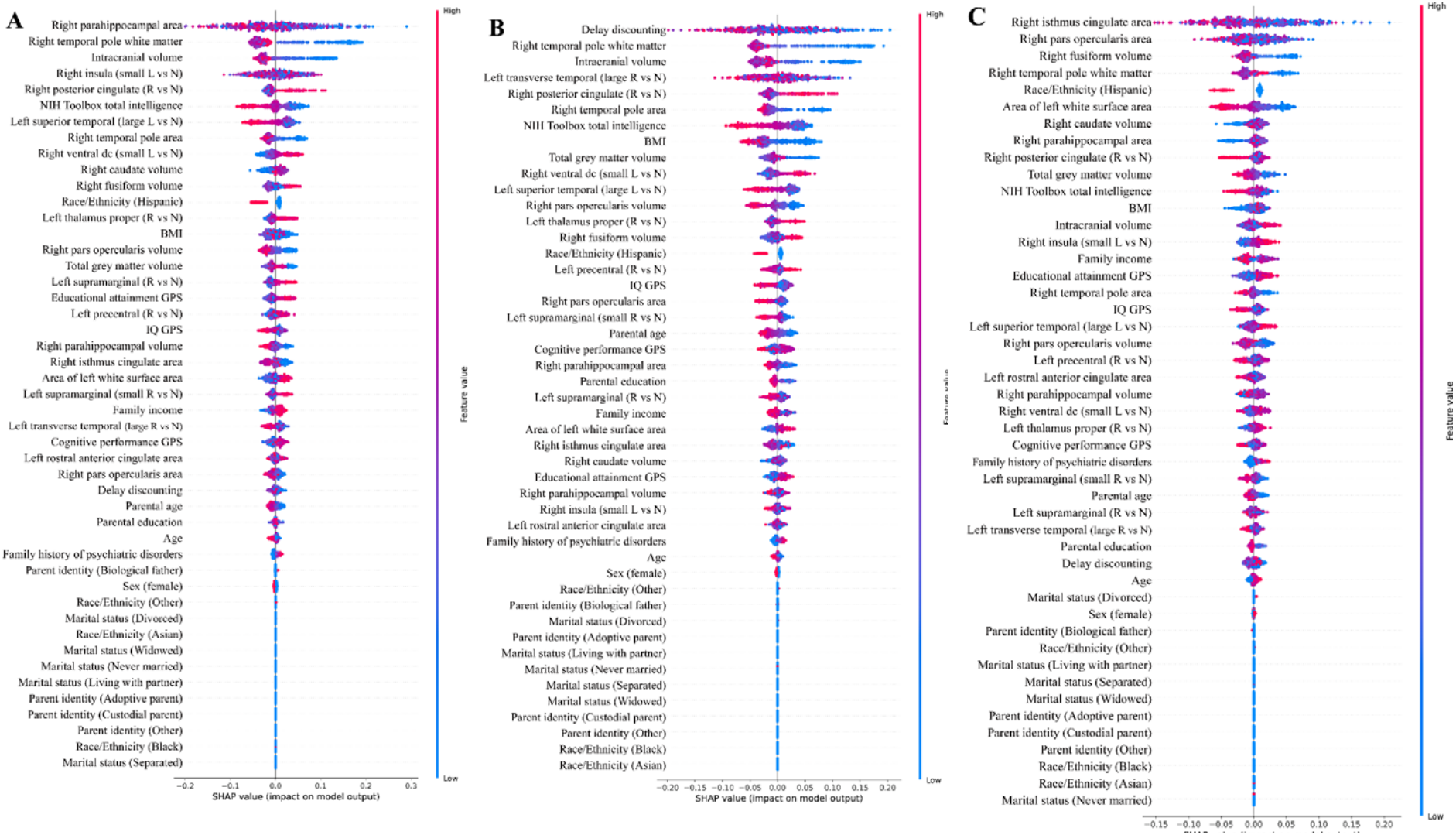

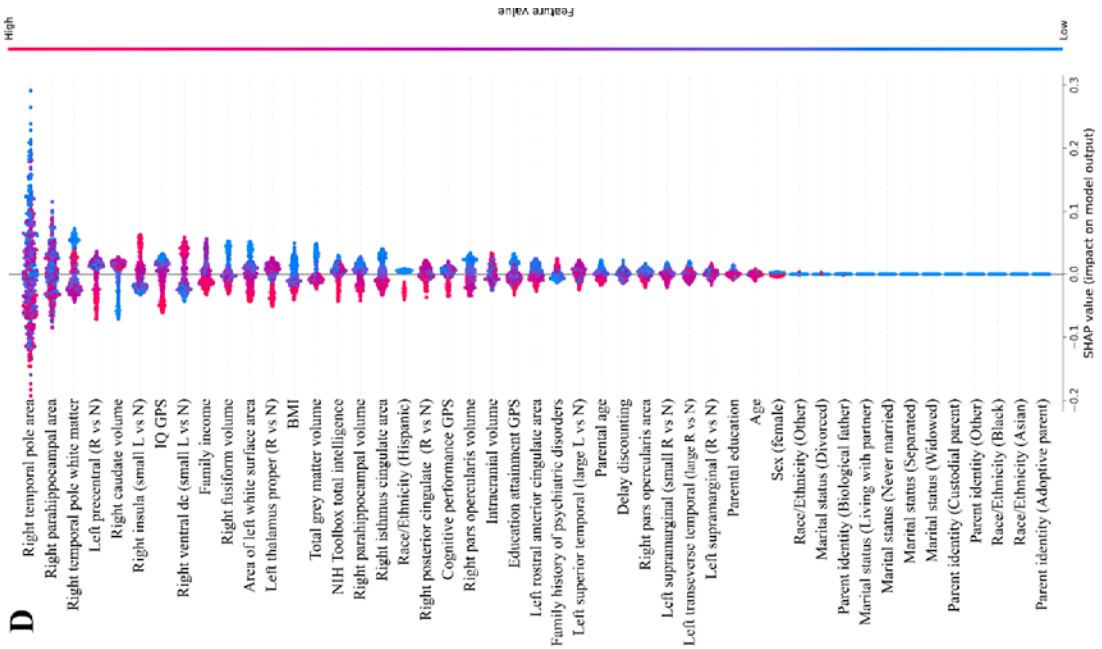

Table S1. Comparison of the sample and national demographics. Since Household income for subjects in the study is presented as deciles, it is transformed into a monetary value by considering the income limits for each decile. The data for the US national demographics is available at Data is available at https://www.census.gov/en.html.

		Mean or Ratio (%)	
		Subjects in our study	**US National Demographics**
Family Income		$70,245	$60,336
Sex	**Male**	53.86%	51.16%
Ethnicity/Race	**White**	65.57%	57.8%
	Black	6.37%	12.1%
	Hispanic	17.47%	18.7%
	Asian	0.33%	6.1%
	Other	10.26%	12.4%

Exploratory analyses using conventional linear IV regression.

In the preliminary exploratory analyses, we conducted a conventional linear IV regression on multiple outcomes, as well as delay discounting and PLEs. Children's neurocognitive ability was measured with uncorrected composite scores of the total, fluid, and crystallized intelligence from the NIH Toolbox Cognitive Battery. The NIH Toolbox is composed of seven cognitive instruments for examining executive function, episodic memory, language abilities, processing speed, working memory, and attention (1, 2). To assess behavioral problems, we used summary scores from the Child Behavior Checklist (CBCL). These included anxious/depressed, withdrawn/depressed, somatic complains, social problems, thought problems, attention problems, rule-breaking behavior, aggressive behavior, obsessive-compulsive problems, sluggish cognitive tempo, stress, internalizing problems score, externalizing problems score, total problems score, and CBCL DSM-5 scales of depression, anxiety disorders, oppositional defiant, conduct problems, and attention deficit/hyperactivity disorder (ADHD) (2, 3). For psychiatric disorders, we used child- and parent-reported Kiddie Schedule for Affective Disorders and Schizophrenia for DSM-5 (KSADS) diagnosis measures (4). Summary scores of anxiety disorder, bipolar disorder, eating disorder, suicidal behavior, and any psychiatric disorders were used.

Table S2. Results of linear IV regression. All p-values were corrected for multiple comparison using false discovery rate.

		Conventional Linear IV Regression				
		Estimates	**Std. Error**	**95% Lower CI**	**95% Upper CI**	**P-FDR**
Delay Discounting		-0.4946	0.2124	-0.9109	-0.0783	0.02
PLEs	Total Score PLE (1-year follow-up)	0.7985	0.2334	0.341	1.256	0.0015
	Distress Score PLE (1-year follow-up)	0.8822	0.2389	0.414	1.3504	0.001
	Total Score PLE (2-year follow-up)	0.6075	0.2188	0.1787	1.0363	0.0069
	Distress Score PLE (2-year follow-up)	0.7472	0.2268	0.3027	1.1917	0.0017
NIH Toolbox	Total Intelligence (Baseline year)	-0.4178	0.4406	-1.2814	0.4458	0.8714
	Fluid Intelligence (Baseline year)	-0.3932	0.4633	-1.3013	0.5149	0.8714

	Crystallized Intelligence (Baseline year)	-0.3881	0.4418	-1.254	0.4778	0.8714
CBCL	Anxious/Depressed (1-year follow-up)	-0.8051	0.5063	-1.7974	0.1872	0.7111
	Withdrawn/Depressed (1-year follow-up)	-0.1604	0.4757	-1.0928	0.772	0.8994
	Somatic Complains (1-year follow-up)	0.8369	0.5092	-0.1611	1.8349	0.7111
	Social Problems (1-year follow-up)	0.1461	0.4756	-0.7861	1.0783	0.9071
	Thought Problems (1-year follow-up)	0.0833	0.4762	-0.85	1.0166	0.9472
	Attention Problems (1-year follow-up)	0.1887	0.4749	-0.7421	1.1195	0.8994
	Rule-breaking Behavior	0.2838	0.4766	-0.6503	1.2179	0.8921

	(1-year follow-up)					
	Aggressive Behavior (1-year follow-up)	0.0965	0.4745	-0.8335	1.0265	0.9468
	Sluggish Cognitive Tempo (1-year follow-up)	-0.3003	0.4816	-1.2442	0.6436	0.8921
	Obsessive-Compulsive Problems (1-year follow-up)	-0.2428	0.4814	-1.1863	0.7007	0.8994
	Stress (1-year follow-up)	-0.4105	0.4775	-1.3464	0.5254	0.8714
	Internalizing Problems (1-year follow-up)	-0.1941	0.4711	-1.1174	0.7292	0.8994
	Externalizing Problems (1-year follow-up)	0.1619	0.4732	-0.7656	1.0894	0.8994
	Total Problems	0.0497	0.4643	-0.8603	0.9597	0.9766

	(1-year follow-up)					
	DSM-5 Depression (1-year follow-up)	0.0444	0.4725	-0.8817	0.9705	0.9766
	DSM-5 Anxiety Disorder (1-year follow-up)	-0.7845	0.5043	-1.7729	0.2039	0.7111
	DSM-5 Somatic Problems (1-year follow-up)	0.6297	0.4978	-0.346	1.6054	0.8714
	DSM-5 ADHD (1-year follow-up)	0.509	0.4857	-0.443	1.461	0.8714
	DSM-5 Oppositional Defiant (1-year follow-up)	-0.1202	0.4778	-1.0567	0.8163	0.9378
	DSM-5 Conduct Problems (1-year follow-up)	0.0937	0.4746	-0.8365	1.0239	0.9468
	Anxious/Depressed	0.1888	0.4784	-0.7488	1.1264	0.8994

	(2-year follow-up)					
	Withdrawn/Depressed (2-year follow-up)	0.6185	0.4979	-0.3574	1.5944	0.8714
	Somatic Complains (2-year follow-up)	0.1816	0.4802	-0.7596	1.1228	0.8994
	Social Problems (2-year follow-up)	1.0335	0.5226	0.0092	2.0578	0.7111
	Thought Problems (2-year follow-up)	-0.0014	0.4746	-0.9316	0.9288	0.9976
	Attention Problems (2-year follow-up)	0.9047	0.5112	-0.0972	1.9066	0.7111
	Rule-breaking Behavior (2-year follow-up)	0.8328	0.5118	-0.1703	1.8359	0.7111
	Aggressive Behavior (2-year follow-up)	0.2914	0.4829	-0.6551	1.2379	0.8921

	Sluggish Cognitive Tempo (2-year follow-up)	-0.035	0.482	-0.9797	0.9097	0.9766
	Obsessive-Compulsive Problems (2-year follow-up)	0.503	0.4902	-0.4578	1.4638	0.8714
	Stress (2-year follow-up)	0.254	0.4796	-0.686	1.194	0.8994
	Internalizing Problems (2-year follow-up)	0.3753	0.4794	-0.5643	1.3149	0.8921
	Externalizing Problems (2-year follow-up)	0.4841	0.4886	-0.4735	1.4417	0.8714
	Total Problems (2-year follow-up)	0.5887	0.4855	-0.3629	1.5403	0.8714
	DSM-5 Depression (2-year follow-up)	0.2878	0.4821	-0.6571	1.2327	0.8921

	DSM-5 Anxiety Disorder (2-year follow-up)	0.2384	0.4801	-0.7026	1.1794	0.8994
	DSM-5 Somatic Problems (2-year follow-up)	-0.3499	0.4907	-1.3117	0.6119	0.8921
	DSM-5 ADHD (2-year follow-up)	0.9614	0.5156	-0.0492	1.972	0.7111
	DSM-5 Oppositional Defiant (2-year follow-up)	0.3292	0.4873	-0.6259	1.2843	0.8921
	DSM-5 Conduct Problems (2-year follow-up)	0.4707	0.4895	-0.4887	1.4301	0.8714
KSADS (Child-reported)	Bipolar Disorder (1-year follow-up)	1.465	0.5858	0.3169	2.6131	0.6875
	Anxiety Disorder (1-year follow-up)	0.4329	0.4944	-0.5361	1.4019	0.8714

	Eating Disorder (1-year follow-up)	-0.2062	0.4906	-1.1678	0.7554	0.8994
	Suicidal Behavior (1-year follow-up)	-0.2188	0.4897	-1.1786	0.741	0.8994
	Sleep Problems (1-year follow-up)	1.1294	0.545	0.0612	2.1976	0.7111
	Any Psychiatric Disorders (1-year follow-up)	0.5648	0.5002	-0.4156	1.5452	0.8714
	Bipolar Disorder (2-year follow-up)	0.3385	0.4912	-0.6242	1.3012	0.8921
	Anxiety Disorder (2-year follow-up)	0.7801	0.5141	-0.2275	1.7877	0.7111
	Eating Disorder (2-year follow-up)	-0.351	0.4951	-1.3214	0.6194	0.8921

	Suicidal Behavior (2-year follow-up)	0.5829	0.5018	-0.4006	1.5664	0.8714
	Sleep Problems (2-year follow-up)	-0.0252	0.4873	-0.9803	0.9299	0.9766
	Any Psychiatric Disorders (2-year follow-up)	0.5595	0.4919	-0.4046	1.5236	0.8714
KSADS (Parent-reported)	Bipolar Disorder (1-year follow-up)	-0.4178	0.4406	-1.2814	0.4458	0.8714
	Anxiety Disorder (1-year follow-up)	-0.3932	0.4633	-1.3013	0.5149	0.8714
	Eating Disorder (1-year follow-up)	-0.3881	0.4418	-1.254	0.4778	0.8714
	Suicidal Behavior (1-year follow-up)	-0.8051	0.5063	-1.7974	0.1872	0.7111

	Sleep Problems (1-year follow-up)	-0.1604	0.4757	-1.0928	0.772	0.8994
	Any Psychiatric Disorders (1-year follow-up)	0.8369	0.5092	-0.1611	1.8349	0.7111
	Bipolar Disorder (2-year follow-up)	0.1461	0.4756	-0.7861	1.0783	0.9071
	Anxiety Disorder (2-year follow-up)	0.0833	0.4762	-0.85	1.0166	0.9472
	Eating Disorder (2-year follow-up)	0.1887	0.4749	-0.7421	1.1195	0.8994
	Suicidal Behavior (2-year follow-up)	0.2838	0.4766	-0.6503	1.2179	0.8921
	Sleep Problems (2-year follow-up)	0.0965	0.4745	-0.8335	1.0265	0.9468

	Any Psychiatric Disorders (2-year follow-up)	-0.3003	0.4816	-1.2442	0.6436	0.8921

Double ML models

To confirm robustness of the IV Forest results, we used double machine learning (Double ML). This up-to-date causal machine learning method can utilize any state-of-the-art machine learning models to obtain consistent, unbiased estimates of average treatment effects by partialling out the confounding effects of covariates (5). It is particularly effective when the covariates are high-dimensional and have complex interactions.

We used partial linear model and nonparametric instrumental variable model. In the partial linear model, we only assume linearity of the treatment variable ADI while the relationships between the outcome variable Y and covariates X and between instrument variable SOI and covariates X remain as an unknown function. On the other hand, the nonparametric model does not require any assumptions specifying the relationship between the outcome Y, treatment ADI, instrument variable SOI, and covariates X. Below shows the simple mathematical representation of each model:

$$Y = \mu ADI + g(X) + \varepsilon, \qquad SOI = m(X) + v \quad (1)$$

$$Y = f(ADI, X) + \varepsilon, \qquad SOI = m(X) + v \qquad (2)$$

Here, Y denote for outcome variable (in our study, delay discounting and psychotic-like experiences), ADI the treatment variable, X multidimensional covariates, SOI the instrument variable. $g(), m(), f()$ are unknown functions and ε, v are random errors. In the partial linear model (Equation 1), we assume that the treatment variable (i.e., ADI) have linear relationship with the outcome variable Y. There are no model assumptions specifying the relationship between multidimensional covariates X, outcome Y, and the instrumental variable SOI. The nonparametric model (Equation 2), on the other hand, does not assume any relationship between the treatment, outcome, covariates, and the instrument. The only required assumption for the nonparametric Double ML model is that the treatment must be a binary variable. Thus, we used ADI as a continuous variable in the partial linear model and a binary variable (i.e., above or below mean) in the nonparametric model.

We built an ensemble machine learning pipeline consisting of elastic net, random forest, XGBoost, support vector machine, and k-Nearest Neighbors with parameters tuned via 5-fold cross validation. In general, ensemble methods can improve model performance with lower error and higher accuracy by combining several base models (6). For each analysis, all continuous variables were standardized (z-scaled) beforehand to obtain standardized estimates, and analyses were run using *DoubleML* (7) packages in R version 4.1.2.

Table S3. Results of Double ML models. All p-values were corrected for multiple comparison using false discovery rate.

	Double ML Partial Linear IV Regression					Double ML Nonparametric IV Regression				
	Estimates	**Std. Error**	**95% Lower CI**	**95% Upper CI**	**P-FDR**	**Estimates**	**Std. Error**	**95% Lower CI**	**95% Upper CI**	**P-FDR**
Delay Discounting (1-year follow-up)	-0.4205	0.1905	-0.7939	-0.0471	0.0273	-0.9002	0.3933	-1.6711	-0.1293	0.0221
Total Score PLE (1-year follow-up)	0.9025	0.1952	0.5199	1.2850	0.0000	1.9331	0.4576	1.0362	2.8299	0.0001
Distress Score PLE (1-year follow-up)	0.8992	0.1970	0.5131	1.2852	0.0000	1.6598	0.4353	0.8065	2.5130	0.0003
Total Score PLE (2-year follow-up)	0.7693	0.1890	0.3990	1.1397	0.0001	1.6563	0.4392	0.7955	2.5171	0.0003
Distress Score PLE (2-year follow-up)	0.7218	0.1829	0.3633	1.0803	0.0001	1.3079	0.4111	0.5021	2.1136	0.0018

Random Forest-based Feature Selection using Boruta

We used Boruta to select GPS and brain ROIs of structural MRI and MID task fMRI significantly associated with delay discounting. Boruta first generates shadow attributes, which is irrelevant to the outcome, by shuffling all input features. It then confirms features that have significantly higher importance in predicting the outcome than the shadow attributes with 95% confidence level, Bonferroni-corrected two-tailed tests (8). The selected features were included as covariates in the IV Forest models for assessing heterogeneous treatment effects of ADI.

Table S4. Results of feature selection with Boruta.

		Boruta Feature Selection					
		meanImp	**medianImp**	**minImp**	**maxImp**	**normHits**	**decision**
GPS	Cognitive performance GPS	9.218585214	9.343664516	1.540057892	14.80316571	0.989218329	Confirmed

	Educational attainment GPS	3.94101317	3.861989404	0.426263498	7.543422156	0.867924528	Confirmed
	IQ GPS (2-year follow-up)	6.797659091	6.806435058	1.974908045	9.841407352	0.994609164	Confirmed
Structural MRI	Left rostral anterior cingulate area	6.414094346	6.475070692	-0.035411504	9.672515329	0.986382979	Confirmed
	Area of the left white surface area	4.947047514	4.993043324	-0.651253674	8.319553071	0.965957447	Confirmed
	Right isthmus cingulate area	3.047499629	3.018073772	-1.525770405	6.367472417	0.748085106	Confirmed
	Right parahippocampal area	3.54003384	3.596050843	-0.735751779	7.584353291	0.847659574	Confirmed
	Right pars opercularis area	2.536130188	2.551497416	-2.732925194	5.521156748	0.596595745	Confirmed
	Right temporal pole	3.646495297	3.642126503	-1.885893836	6.74382961	0.857021277	Confirmed

	area						
	Right fusiform volume	4.8304398	4.820901083	-0.219789984	8.108846062	0.96	Confirmed
	Right parahippocampal volume	2.619089202	2.59585374	-1.650000342	6.456811555	0.644255319	Confirmed
	Right pars opercularis volume	4.904158498	4.939247772	-2.183840684	8.229214003	0.968510638	Confirmed
	Right caudate volume	2.940682064	2.910956975	-1.467310423	6.77699793	0.702978723	Confirmed
	Total grey matter volume	5.225675728	5.237263203	-0.894516992	8.807847283	0.977021277	Confirmed
	Right Temporal pole white matter	6.748279698	6.804387788	0.408403365	9.862430702	0.987234043	Confirmed
MID task fMRI	Left precentral (mean beta: any reward vs neutral)	8.541841922	8.545733335	-0.834551762	12.05424853	0.99719944	Confirmed

	Left supramarginal (mean beta: any reward vs neutral)	8.794762008	8.817520479	-0.407425475	13.13555673	0.99719944	Confirmed
	Right posterior cingulate (mean beta: any reward vs neutral)	10.08222952	10.10382848	-0.002488899	13.94572714	0.99739948	Confirmed
	Left transverse temporal (mean beta: large reward vs neutral)	4.030146815	4.045639319	-1.267815916	7.737267983	0.900780156	Confirmed
	Left supramarginal (mean beta: small reward vs neutral)	7.296523513	7.319216174	0.857396979	11.4804468	0.99739948	Confirmed
	Left superior temporal (mean beta: large loss vs neutral)	2.78080687	2.781792113	-1.254587471	6.827114058	0.683336667	Confirmed
	Right insula (mean beta:	3.418617309	3.43698343	-1.186087206	7.658281079	0.826165233	Confirmed

	small loss vs neutral)						
	Left thalamus proper (mean beta: any reward vs neutral)	7.080539192	7.077726315	-0.078744054	11.13729613	0.99679936	Confirmed
	Right ventral diencephalon (mean beta: small loss vs neutral)	4.40690639	4.397130598	-1.777232203	9.688916388	0.939387878	Confirmed

Table S5. Heterogeneous treatment effects of neighborhood deprivation. Conditional average treatment effects (CATE) in each quintile and the difference between more vulnerable subgroup vs the most resilient subgroup.

	Heterogeneous Treatment Effects				
	Estimates	**Std. Error**	**95% Lower CI**	**95% Upper CI**	**P-FDR**

Total Score PLEs (1-year follow-up)	CATE: Q1	-32.15662482	0.64177702	-33.41448466	-30.89876497	<0.0001
	CATE: Q2	-6.817450066	0.021258615	-6.859116186	-6.775783946	<0.0001
	CATE: Q3	1.184668187	0.006873392	1.171196586	1.198139788	<0.0001
	CATE: Q4	7.091412153	0.014305152	7.063374571	7.119449736	<0.0001
	CATE: Q5	47.45333454	5.043508208	37.5682401	57.33842899	<0.0001
	CATE Q2 – CATE Q1	25.33917475	3.236311588	18.99612059	31.6822289	<0.0001
	CATE Q3 – CATE Q1	33.341293	3.236311588	26.99823885	39.68434716	<0.0001
	CATE Q4 – CATE Q1	39.24803697	3.236311588	32.90498281	45.59109112	<0.0001
	CATE Q5 – CATE Q1	79.60995936	3.226834813	73.28547934	85.93443938	<0.0001
Distress Score PLEs (1-year follow-up)	CATE: Q1	-30.69393828	1.324743622	-33.29038807	-28.0974885	<0.0001
	CATE: Q2	-5.591496226	0.016519156	-5.623873176	-5.559119276	<0.0001
	CATE: Q3	0.645898162	0.00602267	0.634093947	0.657702378	<0.0001
	CATE: Q4	5.339078652	0.011558835	5.316423752	5.361733551	<0.0001
	CATE: Q5	50.4702646	12.1598892	26.63731971	74.30320949	<0.0001
	CATE Q2 – CATE Q1	25.10244206	7.786033177	9.842097448	40.36278667	0.0013

	CATE Q3 – CATE Q1	31.33983645	7.786033177	16.07949184	46.60018106	0.0001
	CATE Q4 – CATE Q1	36.03301694	7.786033177	20.77267233	51.29336155	<0.0001
	CATE Q5 – CATE Q1	81.16420288	7.763233617	65.94854459	96.37986118	<0.0001
Total Score PLEs (2-year follow-up)	CATE: Q1	-36.71170915	2.501408464	-41.61437965	-31.80903865	<0.0001
	CATE: Q2	-7.817465112	0.022331196	-7.861233452	-7.773696772	<0.0001
	CATE: Q3	0.941876877	0.009278149	0.92369204	0.960061715	<0.0001
	CATE: Q4	7.208218093	0.015365381	7.1781025	7.238333686	<0.0001
	CATE: Q5	51.68416443	4.433107643	42.99543311	60.37289575	<0.0001
	CATE Q2 – CATE Q1	28.89424404	3.240112198	22.54374082	35.24474725	<0.0001
	CATE Q3 – CATE Q1	37.65358602	3.240112198	31.30308281	44.00408924	<0.0001
	CATE Q4 – CATE Q1	43.91992724	3.240112198	37.56942403	50.27043045	<0.0001
	CATE Q5 – CATE Q1	88.39587358	3.230624295	82.06396632	94.72778085	<0.0001
Distress Score PLEs (2-year follow-up)	CATE: Q1	-33.13492022	2.654282906	-38.33721912	-27.93262132	<0.0001
	CATE: Q2	-6.914493335	0.018873992	-6.951485679	-6.877500992	<0.0001
	CATE: Q3	0.655325164	0.00868485	0.63830317	0.672347157	<0.0001

	CATE: Q4	5.92002301	0.012630329	5.89526802	5.944778	<0.0001
	CATE: Q5	45.45980748	3.90492866	37.80628795	53.11332702	<0.0001
	CATE Q2 – CATE Q1	26.22042688	3.005525914	20.32970433	32.11114943	<0.0001
	CATE Q3 – CATE Q1	33.79024538	3.005525914	27.89952283	39.68096793	<0.0001
	CATE Q4 – CATE Q1	39.05494323	3.005525914	33.16422068	44.94566577	<0.0001
	CATE Q5 – CATE Q1	78.5947277	2.996724941	72.72125475	84.46820066	<0.0001

Table S6. Heterogeneous treatment effects in the reduced model. Conditional average treatment effects (CATE) in each quintile and the difference between more vulnerable subgroup vs the most resilient subgroup.

		Heterogeneous Treatment Effects				
		Estimates	**Std. Error**	**95% Lower CI**	**95% Upper CI**	**P-FDR**
Total Score PLEs	CATE: Q1	-148.1543362	18.77935701	-184.9611996	-111.3474728	<0.0001

(1-year follow-up)	CATE: Q2	-6.53420787	0.020110819	-6.573624351	-6.494791389	<0.0001
	CATE: Q3	0.96022033	0.007885014	0.944765986	0.975674674	<0.0001
	CATE: Q4	7.404490109	0.016378546	7.372388749	7.436591469	<0.0001
	CATE: Q5	410.1435013	224.347071	-29.56867781	849.8556805	0.0675
	CATE Q2 – CATE Q1	141.6201283	143.3047308	-139.2519829	422.4922395	0.323
	CATE Q3 – CATE Q1	149.1145565	143.3047308	-131.7575547	429.9866677	0.323
	CATE Q4 – CATE Q1	155.5588263	143.3047308	-125.3132849	436.4309375	0.323
	CATE Q5 – CATE Q1	558.2978375	142.8850967	278.248194	838.347481	0.0004
Distress Score PLEs (1-year follow-up)	CATE: Q1	-104.696485	16.64146673	-137.3131604	-72.07980954	<0.0001
	CATE: Q2	-5.536626398	0.017553252	-5.57103014	-5.502222655	<0.0001
	CATE: Q3	0.599742998	0.006478149	0.58704606	0.612439937	<0.0001
	CATE: Q4	5.856716502	0.013778525	5.82971109	5.883721914	<0.0001
	CATE: Q5	118.5487008	28.58248484	62.52805993	174.5693417	<0.0001
	CATE Q2 – CATE Q1	99.15985858	21.05291356	57.89690623	140.4228109	<0.0001
	CATE Q3 – CATE Q1	105.296228	21.05291356	64.03327563	146.5591803	<0.0001

	CATE Q4 – CATE Q1	110.5532015	21.05291356	69.29024913	151.8161538	<0.0001
	CATE Q5 – CATE Q1	223.2451858	20.99126507	182.1030622	264.3873093	<0.0001
Total Score PLEs (2-year follow-up)	CATE: Q1	-85.52329015	4.099782963	-93.55871711	-77.4878632	<0.0001
	CATE: Q2	-7.803896033	0.023027295	-7.849028701	-7.758763364	<0.0001
	CATE: Q3	0.934406516	0.009699511	0.915395824	0.953417208	<0.0001
	CATE: Q4	7.591719182	0.016910888	7.558574451	7.624863912	<0.0001
	CATE: Q5	97.89134501	12.72666057	72.94754865	122.8351414	<0.0001
	CATE Q2 – CATE Q1	77.71939412	8.510983276	61.03817343	94.40061481	<0.0001
	CATE Q3 – CATE Q1	86.45769667	8.510983276	69.77647597	103.1389174	<0.0001
	CATE Q4 – CATE Q1	93.11500933	8.510983276	76.43378864	109.79623	<0.0001
	CATE Q5 – CATE Q1	183.4146352	8.486060871	166.7822615	200.0470088	<0.0001
Distress Score PLEs (2-year follow-up)	CATE: Q1	-119.1798326	12.65102488	-143.9753857	-94.38427946	<0.0001
	CATE: Q2	-6.585759634	0.019441347	-6.623863975	-6.547655293	<0.0001
	CATE: Q3	0.475787123	0.008703222	0.458729122	0.492845125	<0.0001
	CATE: Q4	6.189265297	0.015389133	6.159103151	6.219427443	<0.0001

	CATE: Q5	144.5306933	32.63574853	80.56580159	208.4955851	<0.0001
	CATE Q2 – CATE Q1	112.594073	22.28009232	68.92589443	156.2622515	<0.0001
	CATE Q3 – CATE Q1	119.6556197	22.28009232	75.98744119	163.3237982	<0.0001
	CATE Q4 – CATE Q1	125.3690979	22.28009232	81.70091936	169.0372764	<0.0001
	CATE Q5 – CATE Q1	263.7105259	22.21485033	220.1702193	307.2508325	<0.0001

Table S7. Heterogeneous treatment effects of neighborhood adversity on symptom specific PLEs. Conditional average treatment effects (CATE) in each quintile and the difference between more vulnerable subgroup vs the most resilient subgroup.

		Heterogeneous Treatment Effects				
		Estimates	**Std. Error**	**95% Lower CI**	**95% Upper CI**	**P-FDR**
Delusional Score PLEs	CATE: Q1	-27.60105671	0.829965542	-29.22775928	-25.97435414	<0.0001

(1-year follow-up)	CATE: Q2	-5.021312331	0.013628021	-5.048022762	-4.994601901	<0.0001
	CATE: Q3	0.306832641	0.005911669	0.295245983	0.318419298	<0.0001
	CATE: Q4	4.934784124	0.011629989	4.911989763	4.957578484	<0.0001
	CATE: Q5	39.49057073	4.73923139	30.2018479	48.77929357	<0.0001
	CATE Q2 – CATE Q1	22.57974437	3.062631657	16.57709663	28.58239212	<0.0001
	CATE Q3 – CATE Q1	27.90788935	3.062631657	21.9052416	33.91053709	<0.0001
	CATE Q4 – CATE Q1	32.53584083	3.062631657	26.53319308	38.53848857	<0.0001
	CATE Q5 – CATE Q1	67.09162744	3.053663463	61.10655703	73.07669785	<0.0001
Hallucinational Score PLEs (1-year follow-up)	CATE: Q1	-34.46275535	1.919927574	-38.22574425	-30.69976645	<0.0001
	CATE: Q2	-5.505287059	0.016222743	-5.53708305	-5.473491067	<0.0001
	CATE: Q3	0.576784345	0.00556928	0.565868757	0.587699934	<0.0001
	CATE: Q4	4.790937834	0.010758294	4.769851966	4.812023703	<0.0001
	CATE: Q5	65.58634354	15.81962688	34.5804446	96.59224249	<0.0001
	CATE Q2 – CATE Q1	28.95746829	10.14368045	9.076219942	48.83871664	0.0043
	CATE Q3 – CATE Q1	35.0395397	10.14368045	15.15829135	54.92078805	0.0007

	CATE Q4 – CATE Q1	39.25369319	10.14368045	19.37244483	59.13494154	0.0002
	CATE Q5 – CATE Q1	100.0490989	10.11397708	80.22606809	119.8721297	<0.0001
Delusional Score PLEs (2-year follow-up)	CATE: Q1	-30.28312331	2.961479916	-36.08751729	-24.47872933	<0.0001
	CATE: Q2	-5.096447682	0.015524784	-5.126875701	-5.066019664	<0.0001
	CATE: Q3	0.420575848	0.005192211	0.4103993	0.430752395	<0.0001
	CATE: Q4	4.278131763	0.009950812	4.25862853	4.297634996	<0.0001
	CATE: Q5	39.97828539	3.022560578	34.05417551	45.90239526	<0.0001
	CATE Q2 – CATE Q1	25.18667563	2.69358331	19.90734935	30.4660019	<0.0001
	CATE Q3 – CATE Q1	30.70369916	2.69358331	25.42437288	35.98302543	<0.0001
	CATE Q4 – CATE Q1	34.56125507	2.69358331	29.2819288	39.84058135	<0.0001
	CATE Q5 – CATE Q1	70.2614087	2.685695787	64.99754168	75.52527571	<0.0001
Hallucinational Score PLEs (2-year follow-up)	CATE: Q1	-37.66549065	3.354745615	-44.24067123	-31.09031007	<0.0001
	CATE: Q2	-7.423576439	0.019690386	-7.462168886	-7.384983993	<0.0001
	CATE: Q3	0.573097631	0.011334984	0.550881471	0.59531379	<0.0001
	CATE: Q4	6.537762617	0.013132368	6.512023648	6.563501586	<0.0001

	CATE: Q5	45.91434074	3.974114501	38.12521945	53.70346204	<0.0001
	CATE Q2 – CATE Q1	30.24191421	3.310519318	23.75341557	36.73041284	<0.0001
	CATE Q3 – CATE Q1	38.23858828	3.310519318	31.75008964	44.72708691	<0.0001
	CATE Q4 – CATE Q1	44.20325326	3.310519318	37.71475463	50.6917519	<0.0001
	CATE Q5 – CATE Q1	83.57983139	3.300825244	77.11033279	90.04932999	<0.0001

Mediation Analysis

To test the role of delay discounting as a mediator between ADI and PLEs, we also used a linear mediation analysis. By utilizing *mediation* (9) package in R, we conducted causal mediation analysis by decomposing local average treatment effect (LATE) into local average causal mediation effect (LACME) and local average natural direct effect (LANDE). LACME represents the average hypothetical change in the outcome among compliers when the mediator is changed from the value under the treatment status to the control status while the treatment variable is fixed. LANDE represents the average hypothetical

change in the outcome among compliers when the treatment variable is changed from the treatment status to the control status while the mediator is fixed. In order to control unobserved confounding bias, *ivmediate* function was utilized to incorporate the instrument variable in the causal mediation analysis. In this analysis, ADI and delay discounting were transformed as a binary variable (i.e., above or below mean).

Table S8. Results of conventional linear IV mediation.

		Estimate	95% Lower CI	95% Upper CI
Total score PLE (1year)	**LACME (control)**	-1.526599	-19.800325	15.25005
	LACME (treated)	-0.416918	-4.962959	5.11086
	LANDE (control)	2.506144	-2.827432	6.86333
	LANDE (treated)	3.615825	-12.945040	22.61272
	LATE	2.089226	1.267081	3.36319
Distress score PLE (1year)	**LACME (control)**	-1.389240	-15.157504	18.18372
	LACME (treated)	-0.333498	-4.139243	4.44824

	LANDE (control)	2.102503	-2.521920	6.09491
	LANDE (treated)	3.158245	-15.919809	17.23908
	LATE	1.769005	0.982177	3.06187
Total score PLE (2year)	**LACME (control)**	-0.814506	-10.676019	15.87214
	LACME (treated)	-0.815050	-5.909543	6.61236
	LANDE (control)	2.766819	-4.302505	8.82732
	LANDE (treated)	2.766275	-13.972073	13.81020
	LATE	1.951769	1.164251	3.24240
Distress score PLE (2year)	**LACME (control)**	-0.549539	-8.323329	17.92484
	LACME (treated)	-0.747943	-6.554745	6.70680
	LANDE (control)	2.366669	-4.634207	8.66811
	LANDE (treated)	2.168264	-15.899177	10.35562
	LATE	1.618725	0.887667	2.80599

SI References

1. S. Weintraub *et al.*, Cognition assessment using the NIH Toolbox. *Neurology* **80**, S54-S64 (2013).
2. W. K. Thompson *et al.*, The structure of cognition in 9 and 10 year-old children and associations with problem behaviors: Findings from the ABCD study's baseline neurocognitive battery. *Developmental Cognitive Neuroscience* **36**, 100606 (2019).
3. T. M. Achenbach, T. M. Ruffle, The Child Behavior Checklist and Related Forms for Assessing Behavioral/Emotional Problems and Competencies. *Pediatrics In Review* **21**, 265-271 (2000).
4. J. Kaufman *et al.*, Schedule for Affective Disorders and Schizophrenia for School-Age Children-Present and Lifetime Version (K-SADS-PL): Initial Reliability and Validity Data. *Journal of the American Academy of Child & Adolescent Psychiatry* **36**, 980-988 (1997).
5. V. Chernozhukov *et al.*, Double/debiased machine learning for treatment and structural parameters. *The Econometrics Journal* **21**, C1-C68 (2018).
6. C. Zhang, Y. Ma, *Ensemble Machine Learning: Methods and Applications* (Springer, 2012).
7. P. Bach, V. Chernozhukov, M. S. Kurz, M. Spindler, DoubleML-An Object-Oriented Implementation of Double Machine Learning in Python. *Journal of Machine Learning Research* **23**, 53:51-53:56 (2022).
8. M. B. Kursa, W. R. Rudnicki, Feature Selection with the Boruta Package. *Journal of Statistical Software* **36**, 1 - 13 (2010).
9. D. Tingley, T. Yamamoto, K. Hirose, L. Keele, K. Imai, mediation: R package for causal mediation analysis. *Journal of Statistical Software* **59** (2014).